

THE UNIVERSITY OF WARWICK

Original citation:

Baesens, Claude, Chen, Yi-Chiuan and MacKay, Robert S.. (2013) Abrupt bifurcations in chaotic scattering: view from the anti-integrable limit. *Nonlinearity*, Volume 26 (Number 9). pp. 2703-2730. ISSN 0951-7715

Permanent WRAP url:

<http://wrap.warwick.ac.uk/62379>

Copyright and reuse:

The Warwick Research Archive Portal (WRAP) makes this work by researchers of the University of Warwick available open access under the following conditions.

This article is distributed under the terms of the Creative Commons Attribution 3.0 License (<http://www.creativecommons.org/licenses/by/3.0/>) which permits any use, reproduction and distribution of the work without further permission provided the original work is attributed.

A note on versions:

The version presented in WRAP is the published version, or, version of record, and may be cited as it appears here.

For more information, please contact the WRAP Team at: publications@warwick.ac.uk

warwick**publications**wrap

highlight your research

<http://wrap.warwick.ac.uk/>

Abrupt bifurcations in chaotic scattering: view from the anti-integrable limit

This content has been downloaded from IOPscience. Please scroll down to see the full text.

2013 Nonlinearity 26 2703

(<http://iopscience.iop.org/0951-7715/26/9/2703>)

View [the table of contents for this issue](#), or go to the [journal homepage](#) for more

Download details:

IP Address: 137.205.202.117

This content was downloaded on 07/08/2014 at 14:38

Please note that [terms and conditions apply](#).

Abrupt bifurcations in chaotic scattering: view from the anti-integrable limit*

Claude Baesens¹, Yi-Chiuan Chen² and Robert S MacKay¹

¹ Mathematics Institute, University of Warwick, Coventry CV4 7AL, UK

² Institute of Mathematics, Academia Sinica, Taipei 10617, Taiwan

E-mail: Claude.Baesens@warwick.ac.uk, YCChen@math.sinica.edu.tw and R.S.MacKay@warwick.ac.uk

Received 10 February 2013, in final form 1 July 2013

Published 20 August 2013

Online at stacks.iop.org/Non/26/2703

Recommended by K Ohkitani

Abstract

Bleher, Ott and Grebogi found numerically an interesting chaotic phenomenon in 1989 for the scattering of a particle in a plane from a potential field with several peaks of equal height. They claimed that when the energy E of the particle is slightly less than the peak height E_c there is a hyperbolic suspension of a topological Markov chain from which chaotic scattering occurs, whereas for $E > E_c$ there are no bounded orbits. They called the bifurcation at $E = E_c$ an abrupt bifurcation to chaotic scattering.

The aim of this paper is to establish a rigorous mathematical explanation for how chaotic orbits occur via the bifurcation, from the viewpoint of the anti-integrable limit, and to do so for a general range of chaotic scattering problems.

Mathematics Subject Classification: 37J30, 37J45, 37D05, 70H70

(Some figures may appear in colour only in the online journal)

1. Introduction

Bleher *et al* [7] found numerically an interesting chaotic phenomenon in 1989 when investigating the motion of a particle scattered by a smooth planar potential field $V : \mathbb{R}^2 \rightarrow \mathbb{R}$ of the form

$$V(x, y) = x^2 y^2 \exp(-(x^2 + y^2)). \quad (1)$$



Content from this work may be used under the terms of the [Creative Commons Attribution 3.0 licence](http://creativecommons.org/licenses/by/3.0/). Any further distribution of this work must maintain attribution to the author(s) and the title of the work, journal citation and DOI.

* Dedicated to the memory of Leonid Pavlovich Shilnikov.

When the total energy E of the particle is slightly less than the height $E_c := \max_{(x,y) \in \mathbb{R}^2} V(x,y)$ of the peaks of the potential, their study suggested that there exists a bounded hyperbolic invariant set of the form of a suspension of a Cantor set in the energy level, on which chaotic scattering occurs, whereas there are no bounded orbits when $E > E_c$. If the energy is close to E_c with $E < E_c$, they proposed that the Lyapunov exponents of orbits of the return map to a cross-section of the invariant set are of order $\ln(E_c - E)^{-1}$, while the box-counting dimension of a cross-section to the invariant set is asymptotically proportional to $1/\ln(E_c - E)^{-1}$. They called the bifurcation of dynamics at $E = E_c$ an *abrupt bifurcation* [7]; it is related to a change in the topology of the energy surface.

Potential (1) has four peaks and $\pi/2$ rotation symmetry. In [6], a potential of the form

$$\begin{aligned} V(x,y) &= (x^2 + y^2)^2 \sin^2 \left(\frac{3}{2} \tan^{-1} \frac{y}{x} - \frac{\pi}{4} \right) \exp(-(x^2 + y^2)), \\ &= \frac{r}{2} (r^3 + y^3 - 3x^2y) e^{-r^2}, \quad \text{where } r = x^2 + y^2, \end{aligned} \quad (2)$$

which has three peaks and $2\pi/3$ rotation symmetry, was also studied and much the same bifurcation behaviour was reported. Chaotic scattering from a similar three-hill example had been reported earlier in [26]. The topological entropy of the return map was observed to jump down to 0 as E increases through E_c [23].

In order to explain the aforementioned phenomenon, an argument that invokes [18, 33] on heteroclinic intersection of stable and unstable manifolds of periodic orbits was presented in [6]. There, they numerically verified a sufficient condition that guarantees the intersection. Their analysis, however, falls a long way short of proving the full range of claimed behaviour. In particular their argument does not produce the full topological Markov chain for $E < E_c$, only an unspecified subset, nor does it prove hyperbolicity. Although suggestive, their argument for no bounded orbits when $E > E_c$ is not a proof. In the three-hill case (2) the hills are elliptic, not circular as they assumed, and the analysis of the elliptic case in their section 7 and the later paper [36], although again suggestive, is not complete.

In our paper we develop a general approach to proving chaotic scattering, in particular constructing hyperbolic suspensions of topological Markov chains. Unfortunately, it still does not prove the full extent of the claims of [6], for (1) because of the right angles between the heteroclinic orbits along the edges of the square (a problem already recognized in [6]), and for (2) because the hills are elliptic with their short axes pointing towards the centre whereas we would need the long axes towards the centre to deduce abrupt formation of a topological Markov chain. Nevertheless, we apply our method to deduce a large hyperbolic topological Markov chain for (1) and for two modified three-hill examples.

As already made clear in [6], the dynamics in the vicinity of the peaks of the potential play a crucial role in the bifurcation. Let O be a non-degenerate maximum point of $V : \mathbb{R}^2 \rightarrow \mathbb{R}$. The potential is said to be *elliptic* around O if $D^2V(O)$ has distinct eigenvalues, otherwise it is said to be *circular* around O . The main difference between the dynamics around an elliptic maximum point and a circular one is that trajectories can approach a circular peak in any direction, but can approach an elliptic peak along the long and short axes only, and all but two do so along the long axis. The discussion [6] was primarily for the case where the potential is circular around the peaks, though the elliptic case was considered briefly. For a special setting of potential with large enough non-circularity around a peak, a geometrical sufficient condition for abrupt bifurcation was provided in [36] by analysing the dynamics near the peak, but we shall go well beyond this. For a review on chaotic scattering and its applications, see [30].

The point of our paper is to show that the limit $E \rightarrow E_c$ can be interpreted as a non-degenerate anti-integrable (AI) limit (for this concept, see e.g. [1, 2, 9, 15, 17]) and that a

rigorous analysis is possible in general. It is based on ideas of Turaev and Shilnikov from 1989 [38] for the elliptic case and on [9] for the circular case. Turaev and Shilnikov studied Hamiltonian systems with a hyperbolic equilibrium O_m with a simple pair of eigenvalues of smallest real part and several homoclinic orbits to O_m . One can describe the union of homoclinic orbits as a *bouquet*. They considered the generic case in which the homoclinics leave and return tangent to the slowest eigenvectors of O_m . They showed that for energy just below (or above, respectively) that of O_m there is a subshift of trajectories continuing all concatenations of homoclinics in the bouquet for which at each visit to O_m the direction reverses (stays the same, respectively). Although it is clear they had a strategy in mind, their paper does not contain a proof. A variational proof was provided in [11]. An implicit function theorem version of the result was obtained for the case of circular hills in [9], where the second derivative at the equilibrium has rotation symmetry.

The principal point of our paper is to extend the above to an implicit function theorem proof valid for potentials with more than one local maximum, whether circular or elliptic, provided they all have the same height. Note that, by structural stability of the resulting subshifts, one can perturb the heights by a small amount proportional to the difference of the energy from their mean and still keep the chaotic sets, but cannot expect their creation to be abrupt as the energy is varied.

To complete the analysis one would like to find conditions under which there are no other bounded orbits. This can be done in some circumstances, though even to determine the complete set of homoclinics and heteroclinics to the equilibria is not obvious. We give in this paper two examples, examples 12 and 14 in section 3, for which we are able to prove that there are no bounded orbits when $E > E_c$, the only bounded orbits are the heteroclinics when $E = E_c$, and that there is a (bounded) hyperbolic set of chaotic orbits for all $E \in (E_c - \delta, E_c)$ for some $\delta > 0$.

The rest of this paper is organized as follows. In the next section, we specify the setting, define AI trajectories, and state the main results. In section 3, we recall the non-degeneracy condition for homoclinic and heteroclinic trajectories from [9], and examine their applicability in some examples. In section 4, existence, uniqueness and smooth dependence on the energy of trajectories inside a small neighbourhood of each equilibrium point are studied. In section 5, we define a variational functional which depends on $\epsilon = E - E_c$, and stationary points of which give rise to trajectories of energy E for $\epsilon \neq 0$. In particular, when $\epsilon = 0$ all stationary points of the functional are non-degenerate and correspond to the AI-trajectories. Then we apply the implicit function theorem to continue the AI-trajectories to true trajectories for $\epsilon \neq 0$.

2. Setting and main results

The systems considered in this paper are governed by a Lagrangian of the form

$$L : T\mathbb{R}^2 \rightarrow \mathbb{R}, \quad (x, v) \mapsto L(x, v) = \frac{1}{2}|v|^2 - V(x),$$

where the scalar potential V is C^4 in x and $|\cdot|$ denotes the norm associated to an inner product $\langle \cdot, \cdot \rangle$ on \mathbb{R}^2 . In a future paper we will consider the effects of adding a vector potential. We could allow more general kinetic energy of the form $\frac{1}{2}\langle v, M(x)v \rangle$ with M everywhere positive definite, as arises for general constrained Lagrangian systems, e.g. double pendulum, but in two degrees of freedom, as here, Birkhoff proved this could be reduced to the Euclidean case by change of coordinates and rate of time [5].

The Euler–Lagrange equation is

$$\ddot{x} + \nabla V(x) = 0. \tag{3}$$

We assume the system has properties (V1)–(V3) as follows:

- (V1) There is a finite set O_{\max} of non-degenerate local maximum points for V with equal height E_c , without loss of generality $E_c = 0$ (there can be other local maxima).
- (V2) Each $O \in O_{\max}$ is a hyperbolic equilibrium. Equivalently, the Hessian of V at O is negative definite.
- (V3) There is a finite set $\{\Gamma_k\}_{k \in K}$ of non-degenerate hetero/homoclinic trajectories to O_{\max} (non-degeneracy will be defined in section 3), for some finite index set K , e.g. of integers.

Let

$$p := \frac{\partial L}{\partial v}(x, v) = v$$

be the conjugate momentum. The corresponding Hamiltonian function is

$$H : T^*\mathbb{R}^2 \rightarrow \mathbb{R}, \quad (x, p) \mapsto H(x, p) = \frac{1}{2}|p|^2 + V(x),$$

and the associated Hamilton's equations are

$$\dot{x}_i = p_i, \quad \dot{p}_i = -\frac{\partial V(x)}{\partial x_i}, \quad i = 1, 2.$$

The Hamiltonian is preserved under the Hamiltonian flow, so we have the energy integral

$$E(x, v) = \frac{1}{2}|v|^2 + V(x) = \text{constant}.$$

The equilibrium $(O, 0)$ possesses eigenvalues $\pm\mu_1 = \pm\mu_1(O)$ and $\pm\mu_2 = \pm\mu_2(O)$ with $-\mu_j^2$ the eigenvalues of the Hessian of V at O . Without loss of generality, we take $0 < \mu_1 \leq \mu_2$. The equilibrium is a saddle–saddle equilibrium.

Devaney [20] proved that if an analytic Hamiltonian system possesses a transverse homoclinic orbit to a saddle-focus equilibrium, then for any integer $N \geq 2$ the system admits on the zero energy level a subsystem that is a suspension of the horseshoe with N symbols. In the presence of a gyroscopic force, Buffoni and Séré [13] gave a variational version of Devaney's result using a non-degeneracy condition.

The situation for saddle–saddle equilibria is more subtle, for there are examples where the existence of several transverse homoclinic orbits to a saddle–saddle equilibrium does not imply chaos. See [21] and example 11 to come in section 3. To ensure the occurrence of chaos, additional conditions have to be imposed. For instance, assuming that there are two transverse homoclinic orbits to an elliptic maximum point and some conditions on these orbits, Holmes [29] showed that there is an invariant set on the zero energy level on which the flow is a suspension of a shift automorphism and being hyperbolic it persists to all nearby energies. This contrasts with the scenario of abrupt bifurcation of chaos proposed by [7]. A variational version of his result was given by Berti and Bolle [3]. On the other hand, [38] states that in situations which include that of [29] on the zero energy level, the only orbits which remain forever in a small neighbourhood of the union of the homoclinics are the homoclinics and the equilibrium. Indeed Holmes' chaos is bounded away from the homoclinics.

Nevertheless, [38] also states that chaos is formed for all small enough positive or negative energies, under suitable conditions on homoclinics to a saddle–saddle. This is the direction we follow. The key conditions are non-degeneracy (section 3) and admissibility (definition 1 below).

Let us introduce some notation. Suppose x_1, x_2, x_3 are three points in configuration space for which x_1 is connected to x_2 by a trajectory γ_{12} and x_2 is connected to x_3 by a trajectory γ_{23} . These trajectories are represented by curves. If there is no ambiguity, these curves are still denoted by γ_{12} and γ_{23} . We use the product path $\gamma_{12} \cdot \gamma_{23}$ to represent the concatenation of trajectory curves connecting x_1, x_2 and x_3 in such a way that it starts from x_1 following

γ_{12} to x_2 , then following γ_{23} to x_3 . With this notation, an *anti-integrable (AI) trajectory* is defined to be a bi-infinite product of curves $\cdots \cdot \Gamma_{k_{i-1}} \cdot \Gamma_{k_i} \cdot \Gamma_{k_{i+1}} \cdots$ with $k_i \in K$ and subject to $\lim_{t \rightarrow \infty} \Gamma_{k_i}(t) = \lim_{t \rightarrow -\infty} \Gamma_{k_{i+1}}(t)$ for every $i \in \mathbb{Z}$. Define

$$O_{e_i} = \lim_{t \rightarrow \infty} \Gamma_{k_i}(t) = \lim_{t \rightarrow -\infty} \Gamma_{k_{i+1}}(t) \in O_{\max},$$

and

$$\xi_{k_i}^+ := \lim_{t \rightarrow \infty} \frac{\dot{\Gamma}_{k_i}(t)}{|\dot{\Gamma}_{k_i}(t)|}, \quad \xi_{k_i}^- := \lim_{t \rightarrow -\infty} \frac{\dot{\Gamma}_{k_i}(t)}{|\dot{\Gamma}_{k_i}(t)|}.$$

Definition 1 (Admissibility condition). An AI-trajectory $\cdots \cdot \Gamma_{k_{-1}} \cdot \Gamma_{k_0} \cdot \Gamma_{k_1} \cdots$ or a bi-infinite sequence $\{k_i\}_{i \in \mathbb{Z}}$, $k_i \in K$, is called admissible for $E < 0$ (respectively, $E > 0$) if, for every $i \in \mathbb{Z}$, we have

$$\langle \xi_{k_i}^+, \xi_{k_{i+1}}^- \rangle < 0 \quad (\text{respectively } > 0) \tag{4}$$

when $\mu_1(O_{e_i}) = \mu_2(O_{e_i})$. When $\mu_1(O_{e_i}) \neq \mu_2(O_{e_i})$, besides (4) we require that both $\xi_{k_i}^+$ and $\xi_{k_{i+1}}^-$ are tangent to the eigenvector of $-\mu_1^2$ of the Hessian of V at O_{e_i} .

Remark 2. For $\mu_1(O_{e_i}) \neq \mu_2(O_{e_i})$, the admissibility condition for $E < 0$ (respectively, $E > 0$) admits one situation only:

$$\langle \xi_{k_i}^+, \xi_{k_{i+1}}^- \rangle = -1 \quad (\text{respectively } = 1).$$

We say that a trajectory Υ shadows the AI-trajectory $\cdots \cdot \Gamma_{k_{-1}} \cdot \Gamma_{k_0} \cdot \Gamma_{k_1} \cdots$ if there exists a sequence $\cdots < a_{-1} < b_{-1} < a_0 < b_0 < \cdots$ such that $\Upsilon([b_{i-1}, a_i])$ is contained in a small neighbourhood of Γ_{k_i} and $\Upsilon([a_i, b_i])$ is in a small neighbourhood of O_{e_i} .

The notion of non-degeneracy of a homo/heteroclinic trajectory will be recalled in section 3. We say that an AI-trajectory is non-degenerate if it is made up from non-degenerate homo/heteroclinic trajectories.

Theorem 3. There exists $\epsilon_0 < 0$ such that for any $\epsilon \in (\epsilon_0, 0)$ and any non-degenerate AI-trajectory admissible for $E < 0$ there exists a unique (up to a time shift) trajectory Υ of energy ϵ shadowing such AI-trajectory.

Theorem 4. There exists $\epsilon_1 > 0$ such that for any $\epsilon \in (0, \epsilon_1)$ and any non-degenerate AI-trajectory admissible for $E > 0$ there exists a unique (up to a time shift) trajectory Υ of energy ϵ shadowing such AI-trajectory.

The two theorems above are a corollary of a more detailed result, theorem 23.

By the admissibility condition, the collection of all AI-trajectories over $\{\Gamma_k\}_{k \in K}$ admissible for $E < 0$ (respectively, $E > 0$) determines a topological Markov graph (or subshift of finite type) G_K^- (respectively, G_K^+) with vertices belonging to K . So a bi-infinite sequence $\{\Gamma_{k_i}\}_{i \in \mathbb{Z}}$ is admissible for $E < 0$ (respectively $E > 0$) if and only if the bi-infinite sequence $\{k_i\}_{i \in \mathbb{Z}}$ is admissible by the topological Markov graph G_K^- (respectively, G_K^+).

We shall see that theorem 23 implies that if ϵ is non-zero and sufficiently close to zero, then there is an invariant set Λ_ϵ on the energy level $\{E = \epsilon\}$ on which the dynamics is a suspension of the topological Markov chain G_K^- or G_K^+ . To be precise,

Theorem 5. There exists $\epsilon_0 < 0$ such that for any $\epsilon_0 < \epsilon < 0$ there exists a cross-section $N \in T\mathbb{R}^2$ on the energy level $\{E = \epsilon\}$ for which $\mathcal{A}_\epsilon := N \cap \Lambda_\epsilon$ is a uniformly hyperbolic invariant set with Lyapunov exponents of order $\ln |\epsilon|^{-1}$ for the Poincaré map \mathcal{P}_ϵ . The restriction of \mathcal{P}_ϵ to \mathcal{A}_ϵ is topologically conjugate to the topological Markov chain G_K^- .

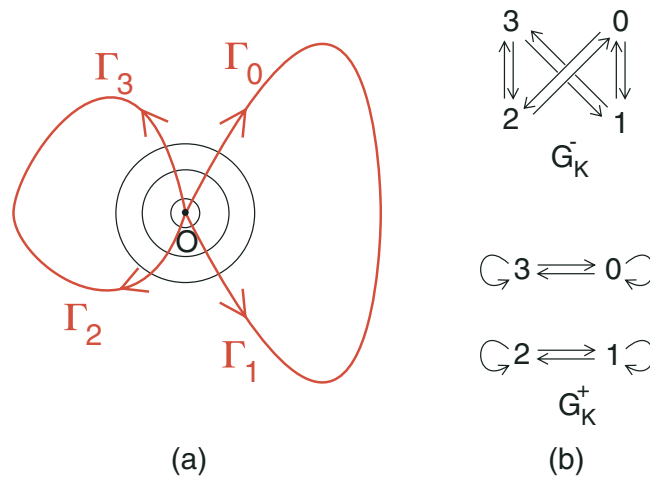


Figure 1. Example 7: (a) homoclinic trajectories to O . (b) Corresponding topological Markov graphs G_K^- and G_K^+ .

Theorem 6. *There exists $\epsilon_1 > 0$ such that for any $0 < \epsilon < \epsilon_1$ there exists a cross-section $N \in T\mathbb{R}^2$ on the energy level $\{E = \epsilon\}$ for which $\mathcal{A}_\epsilon := N \cap \Lambda_\epsilon$ is a uniformly hyperbolic invariant set with Lyapunov exponents of order $\ln |\epsilon|^{-1}$ for the Poincaré map \mathcal{P}_ϵ . The restriction of \mathcal{P}_ϵ to \mathcal{A}_ϵ is topologically conjugate to the topological Markov chain G_K^+ .*

We remark that, by the above two theorems and a result of Fathi [27], the upper box-counting dimension of \mathcal{A}_ϵ is at most of order $1/\ln |\epsilon|^{-1}$.

To illustrate the admissibility condition we give two examples.

Example 7. Suppose the potential V has a non-degenerate circular local maximum point O for which $V(O) = 0$ with four homoclinic trajectories to O , as in figure 1. Denote the homoclinic trajectory traversing clockwise to the right of O by Γ_0 , and the one traversing anti-clockwise to the right of O by Γ_1 (namely the time-reverse of Γ_0). The other two traversing clockwise and anti-clockwise to the left of O are denoted by Γ_2 and Γ_3 , respectively. Let $K = \{0, 1, 2, 3\}$. We obtain the indicated graphs G_K^\pm of admissible transitions for energy above or below 0.

Example 8. Suppose the potential V has three non-degenerate local maxima O_0, O_1 and O_2 with $V(O_0) = V(O_1) = 0$ and $V(O_2) > 0$ as in figure 2. Let $O_{\max} = \{O_0, O_1\}$ (excluding O_2). Suppose O_0 is elliptic and O_1 is circular. Suppose there is a heteroclinic trajectory Γ_0 emanating from O_0 to O_1 and its time-reverse Γ_1 from O_1 to O_0 . Assume there is a homoclinic trajectory Γ_2 to O_1 and a ‘bounce’ time s such that $\Gamma_2(s)$ is not a critical point and that the trajectory meets perpendicularly the level set $V^{-1}(0)$ at $\Gamma_2(s)$. (It is clear that $\ddot{\Gamma}_2(s) \neq 0$, $\dot{\Gamma}_2(s) = 0$, and $\dot{\Gamma}_2(t) \neq 0$ for $-\infty < t \neq s < \infty$; also $\frac{d^2}{dt^2} V(\Gamma_2(s)) < 0$.) Suppose O_1 has two other homoclinic trajectories as in figure 2, Γ_3 traversing clockwise and its time-reverse Γ_4 . Also assume that O_0 has two homoclinic trajectories going out and coming back on opposite sides of the long axis, Γ_5 traversing clockwise and its time-reverse Γ_6 , as in figure 2. Let $K = \{0, 1, 2, 3, 4, 5, 6\}$. We obtain the indicated graphs G_K^\pm of admissible transitions for energy above or below 0.

To apply our theorems to these sorts of example, we need also to verify non-degeneracy hypotheses on the homoclinic or heteroclinic trajectories. We will address this in the next section.

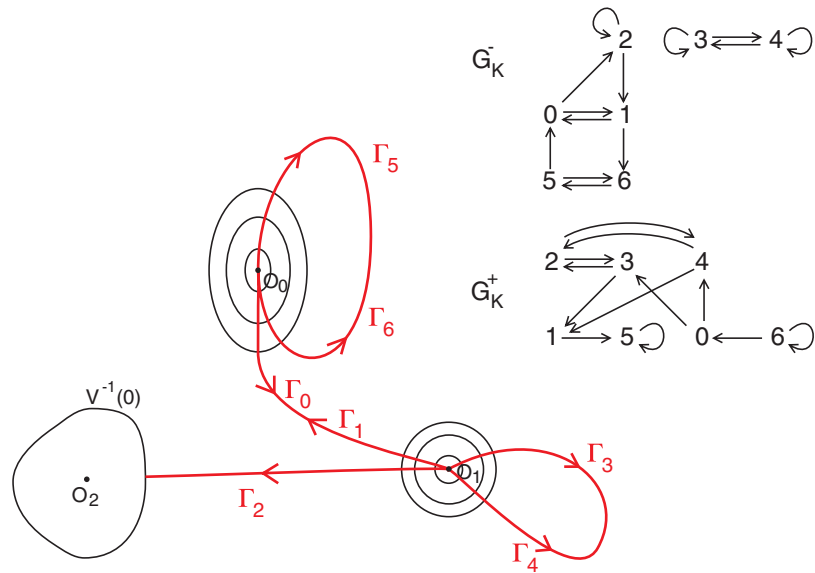


Figure 2. Example 8: heteroclinic and homoclinic trajectories to O_0 and O_1 and topological Markov graphs G_K^- and G_K^+ .

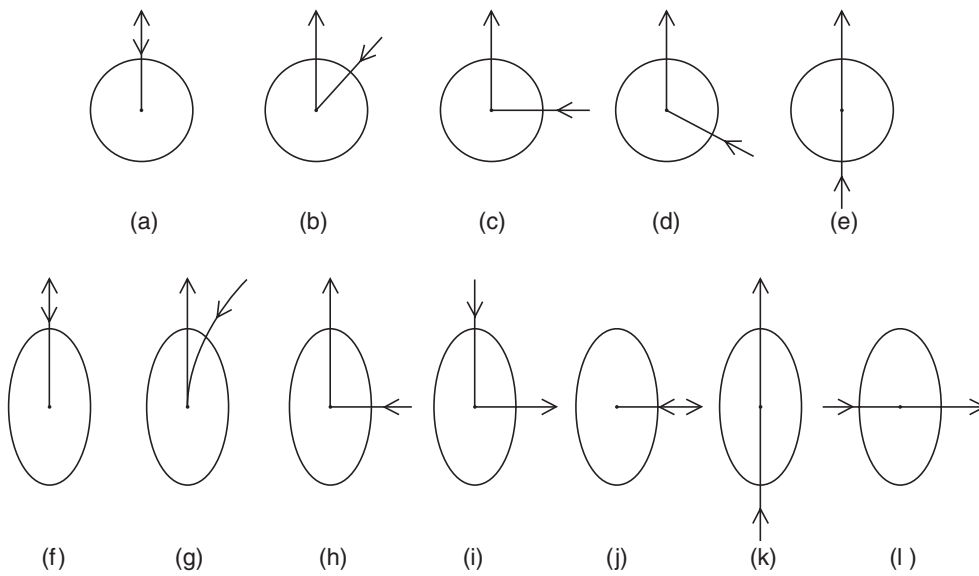


Figure 3. Trajectories asymptotic to a local maximum point O . A circle or ellipse is used to indicate whether the hyperbolic equilibrium $(O, 0) \in T^*\mathbb{R}^2$ has equal or distinct eigenvalues $0 < \mu_1 \leq \mu_2$. The long axis of the ellipse is parallel to the projection of the eigen-direction of μ_1 to the configuration plane. The circle or ellipse also indicates an equipotential curve of the potential V .

We have mentioned that the dynamics in the vicinity of the peaks of the potential V play a crucial role in the bifurcation. Let $O \in O_{\max}$. Depending whether the eigenvalues of $(O, 0) \in T^*\mathbb{R}^2$ are equal or not, there are 12 possibilities for how a pair of trajectories meet at O in the configuration plane as depicted in figure 3. Among them, (a), (b), (f) and (g) fulfil

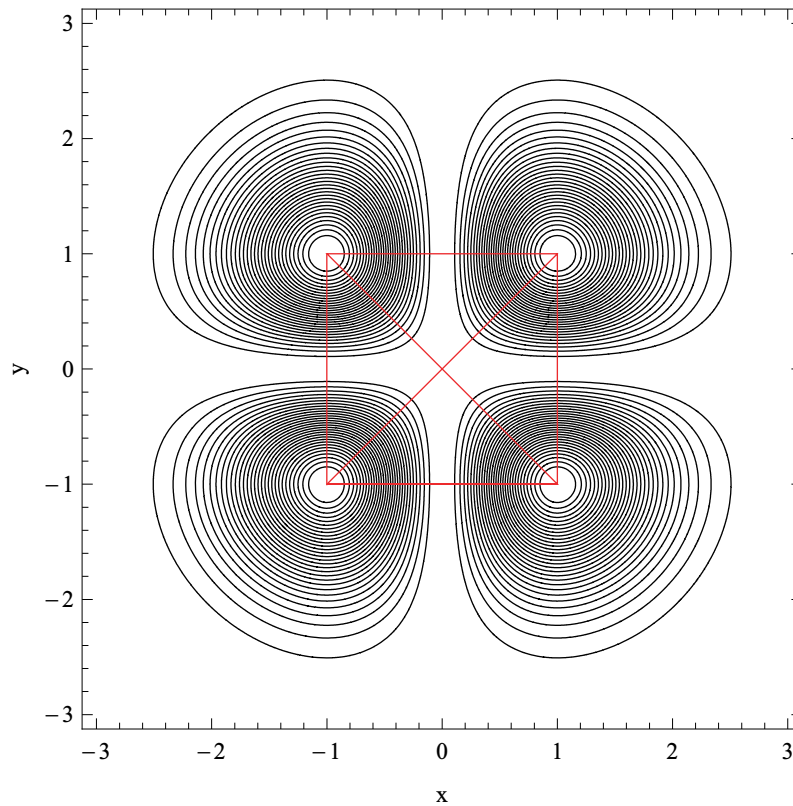


Figure 4. Level sets of the potential V of form (1) and heteroclinics.

the admissibility condition for $E < 0$. Possibilities (d), (e) and (k) fulfil the admissibility condition for $E > 0$. The remaining possibilities (c), (h), (i), (j), and (l) are excluded from our admissibility condition. Some of them have been addressed by [37].

Now we are in a good position to look again at the results of [6, 7]. With the potential of form (1), the straight lines $\{(x, y) \mid x = \pm 1\}$, $\{(x, y) \mid y = \pm 1\}$ and $\{(x, y) \mid y = \pm x\}$ are invariant under the Lagrangian flow (see figure 4). Thus, there are 12 heteroclinic trajectories to the circular maximum points $(\pm 1, \pm 1)$ of the potential (circularity can be proved by direct calculation of the quadratic part; alternatively the sides of the square form orbits and so the reflection symmetry across the diagonal forces the quadratic part to be circular). We prove in example 17 that these heteroclinics are non-degenerate. Hence, by theorem 5, we are able to prove that, when E decreases through $E_c = e^{-2}$, there is an abrupt bifurcation to a subshift Σ on 4 symbols, say 0, 1, 2 and 3, representing the peaks.

We do not, however, obtain the whole of the subshift that Bleher *et al* claim [6], namely that with forbidden words $\{00\}$, $\{11\}$, $\{22\}$ and $\{33\}$, call it Σ_{BGO} . This is because the possibility (c) ('90-degree turn') is not covered by our general approach (it was already perceived as problematic in [6]). Our subshift Σ has forbidden words $\{00\}$, $\{11\}$, $\{22\}$, $\{33\}$, $\{012\}$, $\{123\}$, $\{230\}$, $\{301\}$, $\{032\}$, $\{321\}$, $\{210\}$ and $\{103\}$. The topological entropy of Σ_{BGO} is $\ln 3$, while that of Σ is $\ln(1 + \sqrt{2})$ (this is a relatively simple calculation, based on using symmetry to reduce the equation for the largest eigenvalue of the adjacency matrix for the graph to that for a 2×2 matrix). It is conceivable that the subshift Σ_{BGO} occurs as soon as $E < E_c$, because the shape of the potential might be such that turning 90-degrees is always feasible, though it

would be very weakly hyperbolic for E near E_c . Alternatively, it is possible, indeed likely, that one does not obtain the whole of Σ_{BGO} straightaway. Instead, orbits are probably added gradually to Σ as energy decreases, to make up Σ_{BGO} at some lower energy.

Potential (2) has a maximum point at $(0, \sqrt{2})$, and numerical computation shows that the eigenvalues of the Hessian matrix of the potential there are approximately -1.21802 and -2.16536 (indeed, it is diagonal and easy to show that $V_{xx} \neq V_{yy}$). Hence, the maximum point is elliptic. Its short axis points towards the centre and numerically there are heteroclinics coming in along the long axes (look ahead to figure 8(b)). This means that we cannot deduce an abrupt bifurcation when the energy is lowered through the critical value E_c . Instead the most one can hope for is gradual formation of a full chaotic set as the energy goes sufficiently below E_c so that the dynamics does not notice that the axes are the wrong way round. We did not prove that there are heteroclinic connections, but their existence could be proved by minimizing the Jacobi length of absolutely continuous curves connecting the maximum points inside a bounded region, using compactness and showing the gradient vector ∇V points inwards on the boundary. Furthermore they will come out along the long axes (as in cases (f), (k) in figure 3) because the short axes give only reflection symmetric orbits, which go to infinity. Presumably we could also show that they come in on opposite sides of the maxima as our numerical computation indicates in figure 8(b), but we did not invest time in this. Interestingly, what theorem 4 would give in this setting is two periodic orbits for energy slightly above E_c , rotating in opposite directions round the triangle formed by the heteroclinic connections.

In examples 12 and 14, to come in section 3, we provide two potentials that do exhibit abrupt bifurcation. For these examples, we rigorously prove the existence and non-degeneracy of heteroclinic trajectories, and the absence of bounded trajectories for energy above the maximum. Other examples that could be studied using our results are those of [24, 25].

3. Non-degeneracy conditions and examples

Define

$$M_E := \{x \in \mathbb{R}^2 \mid V(x) \leq E\} \quad (\text{i.e. Hill's region})$$

and let

$$J(\gamma) := \int_0^1 \sqrt{2(E - V(\gamma(s)))} |\dot{\gamma}(s)| ds \quad (5)$$

be the Maupertuis functional on the set $W^{1,1}$ of absolutely continuous curves [14] $\gamma : [0, 1] \rightarrow M_E$ with fixed ends $\gamma(0)$ and $\gamma(1)$. The functional is independent of the parametrization of the curve, and

$$J(\gamma) = \int_\gamma \left\langle \frac{\partial L}{\partial v}(x, v), v \right\rangle dt = \int \langle p, d\gamma \rangle \quad (6)$$

with $v = \dot{\gamma}$, if γ is parametrised in such a way that

$$\frac{|\dot{\gamma}|^2}{2} + V(\gamma) = E. \quad (7)$$

The Maupertuis principle says that if γ is a trajectory of (3) of energy E , then it is a critical point of J , and conversely, any critical point of J becomes a trajectory of energy E after reparametrizing as in (7). Alternatively, one could restrict to energy E by considering critical points of $S = \int_0^\tau (L + E) dt$ with free duration τ . This has the advantage of allowing a more general form of Lagrangian L . Nevertheless we do not need that generality here and furthermore the values of S and J are equal on trajectories of energy E (see section 4).

Suppose $O_e \in O_{\max}$. In the phase space $T^*\mathbb{R}^2$, the hyperbolic equilibrium $(O_e, 0)$ has two-dimensional local stable and unstable manifolds W_{loc}^\pm [31]. Since W_{loc}^\pm are Lagrangian manifolds and locally project diffeomorphically to the configuration plane [28], they are defined by C^2 generating functions S^\pm on a sufficiently small neighbourhood \mathcal{U}_e of O_e :

$$W_{\text{loc}}^\pm = \{(x, p) \mid p = \mp \nabla S^\pm(x), x \in \mathcal{U}_e\}.$$

The functions S^\pm have a non-degenerate minimum at O_e ; without loss of generality $S^\pm(O_e) = 0$.

For any $x \in \mathcal{U}_e$, there exists a unique trajectory $\omega_x^+ : [0, \infty) \rightarrow \mathcal{U}_e$ such that $\omega_x^+(0) = x$ and $\lim_{t \rightarrow \infty} \omega_x^+(t) = O_e$. Similarly, there exists a unique trajectory $\omega_x^- : (-\infty, 0] \rightarrow \mathcal{U}_e$ such that $\omega_x^-(0) = x$ and $\lim_{t \rightarrow -\infty} \omega_x^-(t) = O_e$. Then,

$$S^+(x) = \int_0^\infty L(\omega_x^+(t), \dot{\omega}_x^+(t)) dt,$$

$$S^-(x) = \int_{-\infty}^0 L(\omega_x^-(t), \dot{\omega}_x^-(t)) dt.$$

Remark that $S^+(x)$ is equal to $S^-(x)$ due to time reversibility of the system.

For $x \in \mathcal{U}_e$, the Maupertuis action J of the trajectory ω_x^+ (for energy 0) is $S^+(x)$ using (6). Similarly that of ω_x^- is $S^-(x)$.

Take $\delta > 0$ small enough so that defining

$$U_{e,\delta} = \{x \in \mathcal{U}_e \mid S^\pm(x) < \delta\}, \tag{8}$$

then $S^\pm(x) = \delta$ for all $x \in \partial U_{e,\delta}$. We write $U_e = U_{e,\delta}$. Its boundary ∂U_e is C^2 and for all $x \in \partial U_e$, ω_x^\pm intersect ∂U_e orthogonally, by the first variation formula, see [8, 12].

Suppose δ is sufficiently small and $O_{e_0}, O_{e_1} \in O_{\max}$. Let

$$\begin{aligned} \Pi &= \Pi(M_0, \partial U_{e_0}, \partial U_{e_1}) \\ &:= \{\tilde{\gamma} : [0, 1] \rightarrow \overline{M_0} \mid \tilde{\gamma}(0) \in \partial U_{e_0}, \tilde{\gamma}(1) \in \partial U_{e_1}\} \end{aligned}$$

be the space of absolutely continuous curves with endpoints in ∂U_{e_0} and ∂U_{e_1} .

For any $\tilde{\gamma} \in \Pi$ with $\tilde{\gamma}(0) = y$ and $\tilde{\gamma}(1) = x$, define a curve γ by adding two segments ω_y^- and ω_x^+ . (We also need to reparametrize the curve so that $\gamma(0) = O_{e_0}$ and $\gamma(1) = O_{e_1}$.) Following [8], for any critical point $\tilde{\gamma}$ of the functional J on Π , the curve γ is a hetero/homoclinic trajectory provided γ is reparametrized as (7). Moreover, $J(\gamma) = J(\tilde{\gamma}) + 2\delta$.

The condition that γ is non-degenerate can be expressed in the following equivalent ways.

- (1) γ is a non-degenerate critical point of the Maupertuis functional $J : \Omega \rightarrow \mathbb{R}$ on the subset of curves with the parametrization (7), where

$$\Omega = \Omega(M_0, O_{e_0}, O_{e_1}) = \{\gamma : [0, 1] \rightarrow M_0 \mid \gamma(0) = O_{e_0}, \gamma(1) = O_{e_1}\}$$

is the space of absolutely continuous curves with fixed boundary points O_{e_0} and O_{e_1} .

- (2) γ is the concatenation $\omega_{\tilde{\gamma}(0)}^- \cdot \tilde{\gamma} \cdot \omega_{\tilde{\gamma}(1)}^+$ and $\tilde{\gamma}$ is a non-degenerate critical point of the Maupertuis functional $J : \Pi \rightarrow \mathbb{R}$ on the subset of curves with the parametrization (7).
- (3) Any point $(\tilde{\gamma}, \tau) \in \Pi \times \mathbb{R}^+$ defines a curve $\tilde{u} : [0, \tau] \rightarrow \overline{M_0}$ by $\tilde{u}(t) = \tilde{\gamma}(t/\tau)$. Let

$$G(\tilde{u}, \tau) = \int_0^\tau L(\tilde{u}(t), \dot{\tilde{u}}(t)) dt$$

be its action. Then γ is non-degenerate if $\gamma = \omega_{\tilde{\gamma}(0)}^- \cdot \tilde{\gamma} \cdot \omega_{\tilde{\gamma}(1)}^+$ and (\tilde{u}, τ) is a non-degenerate critical point for G .

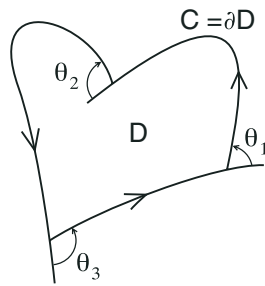


Figure 5. A simple closed curve formed by three pieces of trajectories. The angles turned are measured anti-clockwise, similarly to the external angles of a polygon.

- (4) Define $u : \mathbb{R} \rightarrow M_0$ satisfying $\lim_{t \rightarrow -\infty} u(t) = O_{e_0}$ and $\lim_{t \rightarrow \infty} u(t) = O_{e_1}$ with the parametrization (7) obtained from a critical point γ of the Maupertuis functional. Then γ is non-degenerate if the unique (up to a scalar multiple) solution ξ of the linearized Euler–Lagrange equation along the hetero/homoclinic trajectory u satisfying $\lim_{t \rightarrow \pm\infty} \xi(t) = 0$ is \dot{u} .

We will find it convenient to use the following sufficient (but not necessary) condition for non-degeneracy. Equipped with the Jacobi metric $\sqrt{2(E - V(x))} |dx|$, geodesics in Hill’s region M_E are trajectories of the Lagrangian system with potential V and energy E , and vice versa. The Jacobi metric is a Riemannian metric which degenerates on the boundary ∂M_E . The Gaussian curvature $K_E(x)$ of x in M_E is

$$\begin{aligned} K_E(x) &= -\frac{1}{4} \frac{\Delta \ln(E - V(x))}{E - V(x)} \\ &= \frac{1}{4} \left(\frac{\Delta V(x)}{(E - V(x))^2} + \frac{|\nabla V(x)|^2}{(E - V(x))^3} \right), \end{aligned} \quad (9)$$

where Δ is the Laplacian operator, that is, $\Delta V(x)$ means the trace of the Hessian of V . To show a heteroclinic γ is non-degenerate it suffices that the Gaussian curvature in a neighbourhood of $\{\gamma(t) \mid 0 < t < 1\}$ be negative.

The following result, which will be useful later for proving absence of bounded trajectories for $E > E_c$ in examples 12 and 14, is a Jacobi metric version of the Gauss–Bonnet formula. (See figure 5.)

Theorem 9 (The Gauss–Bonnet formula). *Suppose C is a simple closed piecewise smooth curve consisting of m pieces of trajectories ($m \geq 1$). Let $\theta_1, \theta_2, \dots, \theta_m$ be the angle turned at each point where there is a velocity discontinuity. Then*

$$\pm 2 \iint_D K_E(x)(E - V(x)) \, dS + \sum_{i=1}^m \theta_i = \pm 2\pi,$$

with plus sign if C is anti-clockwise, or minus sign otherwise, where D is the region bounded by C .

Proof. The curvature $\kappa(x)$ of a trajectory is given by

$$\begin{aligned} \kappa(x) &= \frac{\nabla_{\perp} V(x)}{|\dot{x}|^2} \\ &= \frac{\nabla_{\perp} V(x)}{2(E - V(x))} \\ &= -\frac{1}{2} \nabla_{\perp} \ln(E - V(x)), \end{aligned}$$

where $\nabla_{\perp} V(x)$ means $\nabla V(x) \cdot \hat{n}$ with \hat{n} the unit tangent vector perpendicular to \dot{x} satisfying $\hat{n} \times \dot{x} = |\dot{x}| \hat{k}$ (in the usual $(\hat{i}, \hat{j}, \hat{k})$ -Euclidean coordinates). Suppose $C = \gamma_1 \cdot \gamma_2 \cdots \gamma_m$ is a product of m pieces of trajectories, with $\gamma_1 = \{x_1(t) \mid t_1^0 \leq t \leq t_1^1\}$, $\gamma_2 = \{x_2(t) \mid t_2^0 \leq t \leq t_2^1\}$, etc. Then by Green's theorem the angle turned by these trajectories along C is $\pm 2\pi - \sum_{i=1}^m \theta_i$:

$$\begin{aligned} \pm 2\pi - \sum_{i=1}^m \theta_i &= \int_{t_1^0}^{t_1^1} \kappa(x_1) |\dot{x}_1| dt + \cdots + \int_{t_m^0}^{t_m^1} \kappa(x_m) |\dot{x}_m| dt \\ &= \int_C \kappa(x) |dx| \\ &= -\frac{1}{2} \int_C \nabla_{\perp} \ln(E - V(x)) |dx| \\ &= \mp \frac{1}{2} \iint_D \Delta \ln(E - V(x)) dS \\ &= \pm 2 \iint_D K_E(x) (E - V(x)) dS, \end{aligned} \tag{10}$$

where dS is an element of surface area in D , and (10) takes the minus sign if the trajectory traverses C anti-clockwise, the plus sign otherwise. \square

Corollary 10. *Suppose K_E is non-positive.*

- (i) *Any trajectory of energy E cannot self-intersect.*
- (ii) *Any two distinct trajectories of energy E can intersect at most once.*

Example 11.

- (a) For the system of two uncoupled pendula

$$\begin{aligned} L((x_1, x_2), (\dot{x}_1, \dot{x}_2)) &= \frac{1}{2}(\dot{x}_1^2 + \dot{x}_2^2) - (\cos 2\pi x_1 - 1) - (\cos 2\pi x_2 - 1), \\ (x_1, x_2) &\in \mathbb{R}^2 / \mathbb{Z}^2, \end{aligned}$$

there are four non-degenerate homoclinic trajectories to $(0, 0)$, along the sides of the unit square in both directions, and a continuum of degenerate homoclinic orbits from one corner to the diagonally opposite one, see [3, 11]. Any pair of non-degenerate homoclinics joining at $(0, 0)$ behave like case (c) or (e) in figure 3.

- (b) Similarly, all except four homoclinic trajectories to $(0, 0)$ for the Lagrangian

$$L((x_1, x_2), (\dot{x}_1, \dot{x}_2)) = \frac{1}{2}(\dot{x}_1^2 + \dot{x}_2^2) + x_1^2 - x_1^4 + 2x_2^2 - 2x_2^4, \quad (x_1, x_2) \in \mathbb{R}^2$$

are degenerate. Any pair of non-degenerate homoclinic orbits joining at the origin behave like case (h), (i), (k) or (l) in figure 3.

Example 12. The Lagrangian system with potential

$$V(x, y) = -3x^2y + y^3 - (x^2 + y^2)^2$$

(see figure 6(a)) has the following properties:

- (o) V has three maxima $(0, 3/4)$, $(-3\sqrt{3}/8, -3/8)$ and $(3\sqrt{3}/8, -3/8)$, and they are elliptic with long axes towards the origin.
- (i) There exist precisely 6 heteroclinic trajectories between the maxima. They are confined to the equilateral triangle with vertices the three maxima. Their connections behave like case (g) in figure 3.

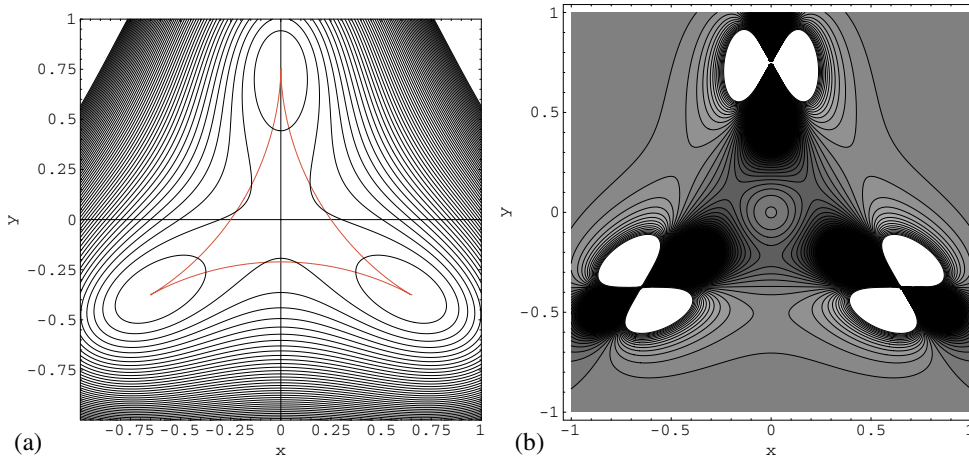


Figure 6. (a) Level sets of the potential V in example 12 and heteroclinics forming a cusped triangle. (b) Level sets of the curvature $K_{27/256}$ with value below 100. Darker shading indicates negative curvature, lighter shading indicates positive curvature, and the level set of zero curvature is the three straight lines through the hilltops plus the origin. Note that for each potential hill top there are two sectors of approach in which the curvature is positive and two in which it is negative.

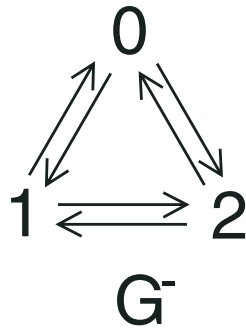


Figure 7. Markov graph G^- for examples 12 and 14.

- (ii) All the heteroclinic trajectories are non-degenerate.
- (iii) For any energy E , all bounded trajectories are confined to the equilateral triangle.
- (iv) For $E > E_c = 27/256$, there are no bounded trajectories.
- (v) For $E = E_c$, the only bounded trajectories are the equilibria and heteroclinics between them.
- (vi) There is $\delta > 0$ such that for all $E \in (E_c - \delta, E_c)$ there is a hyperbolic suspended subshift corresponding to the Markov graph G^- of figure 7.

Proof.

- (o) To find the maxima is simple calculus. The eigenvalues of the Hessian matrix of the potential evaluated at the maxima are $-27/4$ and $-9/4$, thus the maxima are elliptic.
- (i) Minimize the Jacobi length from one maximum to another over the set of absolutely continuous curves contained in the equilateral triangle. The minimum is achieved, by compactness of the set. The result is a geodesic provided it does not include any segment on the boundary. Suppose there is a segment on the lower boundary $\{(x, y) \mid |x| < 3\sqrt{3}/8, y = -3/8\}$. But $\frac{\partial}{\partial y}(E - V) < 0$ in the region $4(x^2 + y^2)y < 3(y^2 - x^2)$

which includes the lower boundary. So we can achieve a reduction in the Jacobi length by pushing the curve into the interior of the triangle. Because the eigenvectors of the smaller eigenvalue point to the centre of the triangle, the heteroclinics meet at any of the maximum points like case (g) in figure 3. The heteroclinic orbit from one maximum to another is unique by the hyperbolicity to be shown in (ii) and the constraint (v) that they must lie in the triangle. The six heteroclinics found numerically are illustrated in figure 6(a) (they occur in pairs in opposite directions).

- (ii) It suffices to show that the Gaussian curvature is negative in the interior of the equilateral triangle minus the origin (which the heteroclinics do not visit). Direct calculation shows that

$$K_{27/256}(x, y) = -\frac{(x^2 + y^2)(\frac{3}{8} + y)(\frac{3}{4} + \sqrt{3}x - y)(\frac{3}{4} - \sqrt{3}x - y)}{2(\frac{27}{256} + 3x^2y - y^3 + (x^2 + y^2)^2)^3}.$$

Thus, the zero set of the curvature consists of the three straight lines through the maxima plus the origin, and the curvature is negative inside the triangle, except at the centre. The curvature has a singularity at the maximum points. See figure 6(b).

- (iii) We show that for any E , any trajectory that leaves the equilateral triangle will go to infinity. For the region $\{0 \leq x \leq -\sqrt{3}y, y \leq -3/8\}$, a simple calculation shows that

$$\begin{aligned} \frac{\partial V(x, y)}{\partial y} &= -3x^2 + 3y^2 - 4y(x^2 + y^2) \\ &\geq -3x^2 + x^2 + 4\frac{3}{8}\left(x^2 + \frac{x^2}{3}\right) \\ &\quad \text{(with equality only if } (x, y) = (3\sqrt{3}/8, -3/8) \\ &= 0. \end{aligned}$$

So the force has negative vertical component in the region. When a particle leaves the triangle from a point on the segment $\{0 \leq x \leq 3\sqrt{3}/8, y = -3/8\}$, the vertical component of its velocity must be non-positive. Hence, the vertical component of the particle's velocity will always stay negative and bounded away from zero. Therefore, the particle goes to infinity. (For trajectories that cross the lines $\{x = 0\}$ or $\{y = -x/\sqrt{3}\}$, use the symmetry of the system.)

- (iv) We have shown that $K_{27/256}(x) < 0$ when x is in the interior of the equilateral triangle minus the origin. It follows that $K_E(x) < 0$ for all x in the triangle when $E > E_c = 27/256$. To see this, $K_{27/256}(x) < 0$ implies from (9) that $(E_c - V)\Delta V \leq -|\nabla V|^2$ at x , which implies that $(E - V)\Delta V < -|\nabla V|^2$ at x for all $E > E_c$ (because $E_c > V(x)$ so $\Delta V < 0$). Suppose there is a bounded trajectory γ . It has to lie within the triangle, so must have an accumulation point in phase space (since the part of the energy level that projects to the configuration space in the triangle is compact). The accumulation point cannot be an equilibrium because $E > E_c$. This implies that there is $\mu \geq 0$ and $t_1 < t_2$ such that $\max\{|\gamma(t_2) - \gamma(t_1)|, |\dot{\gamma}(t_2) - \dot{\gamma}(t_1)|\} < \mu$ (the velocity at $\gamma(t_1)$ and $\gamma(t_2)$ are in almost the same direction). If μ is zero, γ is a periodic trajectory, contradicting (i) of corollary 10. If μ is not zero, one can take μ sufficiently small so that there is a segment ν of another trajectory connecting $\gamma(t_1)$ and $\gamma(t_2)$. (This can be done since $E > E_c$.) The two segments $\{\gamma(t) \mid t_1 \leq t \leq t_2\}$ and ν form a simple closed curve since γ cannot self-intersect (by (i) of corollary 10). But, this contradicts (ii) of the corollary. (Remark: alternatively, one can prove this assertion by proposition 13.)
- (v) The equilateral triangle can be decomposed into six right triangles of the same area and shape (up to translation and rotation). One of them is $\{0 \leq x \leq -\sqrt{3}y, -3/8 \leq y \leq 0\}$.

In this one, we have

$$\frac{\partial^2 V}{\partial y \partial x}(x, y) = -2x(3 + 4y) \leq 0,$$

with the last equality only when $x = 0$. And

$$\frac{\partial V}{\partial x}\left(x, \frac{-x}{\sqrt{3}}\right) = -2x^2 \left(-\sqrt{3} + \frac{8}{3}x\right) \geq 0$$

on the hypotenuse $\{(x, y) \mid 0 \leq x \leq 3\sqrt{3}/8, \sqrt{3}y = -x\}$, with the last equality only when $x = 0$ or $x = 3\sqrt{3}/8$. This means that in the interior of the right triangle the force always has negative horizontal component, and implies that a particle in the interior must go to and cross the boundary of the right triangle unless it is asymptotic to the maximum point $(3\sqrt{3}/8, -3/8)$. If its trajectory is asymptotic to the maximum point, then consider it in the opposite time direction. If in the opposite time direction it is also asymptotic to a maximum point, it is a heteroclinic. It cannot be a homoclinic because then it would contain a loop, thus it, or another homoclinic by symmetry of the system, must have a point with zero horizontal velocity. (The case like Γ_2 in figure 2(a) cannot happen here). Due to the negative horizontal force, the particle cannot go the maximum point. When the particle crosses the lower boundary $\{(x, y) \mid 0 \leq x \leq 3\sqrt{3}/8, y = -3/8\}$, it has to go to infinity. When it crosses the side $\{(x, y) \mid x = 0, -3/8 \leq y \leq 0\}$ or the hypotenuse to another right triangle, by (ii) of corollary 10, it cannot come back to the original right triangle. Hence, the particle will cross the segment $\{(x, y) \mid x = 0, -3/8 \leq y \leq 0\}$ twice or cross the boundary of the equilateral triangle. The former case contradicts (ii) of corollary 10, while the latter results in an unbounded trajectory.

Part (vi) is a consequence of theorem 3. \square

Proposition 13. *For $E > E_c$, if there is a bounded trajectory γ in the configuration space there is one with a self-intersection.*

Proof. Let Γ be the phase space orbit corresponding to γ . Γ is bounded so take a limit point A of Γ and its orbit Γ' . Then Γ' consists of limit points of Γ , so is bounded. If it has no self-intersections, take a limit point B . Denote the projections to configuration space of all the above by the corresponding lower case letters. The velocity in configuration space is non-zero at b because $E > E_c$. Take a local transverse section σ through b . Then γ' cuts σ repeatedly and these intersections are themselves limit points of γ . As in the proof of the Poincaré-Bendixson theorem, successive intersections of a non-self-intersecting trajectory with σ are monotonic and thus γ' forms a closed curve, which contradicts its having no self-intersections. \square

Example 14. The Lagrangian system with potential

$$V(x, y) = -3x^2y + y^3 - (x^2 + y^2)^3$$

(figure 8) has the following properties:

- (o) V has three maxima $(0, 2^{-1/3})$, $(-2^{-4/3}\sqrt{3}, -2^{-4/3})$ and $(2^{-4/3}\sqrt{3}, -2^{-4/3})$ and they are circular.
- (i) There exist exactly six heteroclinic trajectories between the maxima and their connections behave like case (b) in figure 3.
- (ii) All the heteroclinic trajectories are non-degenerate.

- (iii) For any energy E , all bounded trajectories are confined to the equilateral triangle with vertices the three maxima.
- (iv) For $E > E_c = 1/4$, there are no bounded trajectories.
- (v) For $E = E_c$, the only bounded trajectories are the equilibria and the heteroclinics between them.
- (vi) There is $\delta > 0$ such that for all $E \in (E_c - \delta, E_c)$ there is a hyperbolic suspended subshift based on the graph of figure 7.

Proof.

- (o) To find the maxima is simple calculus. The eigenvalues of the Hessian of the potential at the maximum points are double, equal to $-9/2^{1/3}$, thus the peaks are circular.
- (ii) On the energy level $\{E = 1/4\}$, trajectories of the Lagrangian system are geodesics of the Jacobi metric $\sqrt{2(E - V(x, y))} |d(x, y)|$. Let $z = x + iy$. Then in the complex z -plane the metric can be written as $\rho(z)|dz|$ with

$$\rho(z) = |\sqrt{2}z^3 + i/\sqrt{2}|.$$

Note that the metric degenerates only at the hilltops $z_1 = 2^{-1/3}e^{i\pi/2}$, $z_2 = 2^{-1/3}e^{i7\pi/6}$ and $z_3 = 2^{-1/3}e^{i11\pi/6}$. Furthermore, the metric $\rho(z)|dz|$ corresponds to the Euclidean metric $|dw|$ in the w -plane where

$$w(z) = \sqrt{2}z^4/4 + iz/\sqrt{2}. \tag{11}$$

Since all geodesics in the w -plane with the metric $|dw|$ are Euclidean straight lines, all trajectories for the Lagrangian system are non-degenerate.

- (i) Note that heteroclinics correspond to the straight lines joining the three points $w(z_1)$, $w(z_2)$ and $w(z_3)$, thus can be obtained by solving the quartic equation (11) for z and choosing the right solution. (See figure 8(a)). Points z_1 , z_2 and z_3 are located at the vertices of an equilateral triangle. The mapping $z \mapsto w$ has $2\pi/3$ rotation symmetry, thus $w(z_1)$, $w(z_2)$ and $w(z_3)$ are also located at the vertices of an equilateral triangle. Taking Taylor expansion around z_1 , z_2 and z_3 , we see that the heteroclinics meet at an angle of $\pi/6$ at z_1 , z_2 or z_3 .
- (iii) Note that

$$\frac{\partial}{\partial y} V(x, y) = -3x^2 + 3y^2 - 6y(x^2 + y^2)^2,$$

and

$$-\frac{\partial}{\partial y} V(x, -2^{-4/3}) = -3 \times 2^{-1/3}(x^2 - 3 \times 2^{-8/3})^2.$$

The latter is negative except when x is at a maximum point. The second partial derivative

$$\frac{\partial^2}{\partial y^2} V(x, y) = 6y - 6(x^2 + y^2)^2 - 24y^2(x^2 + y^2)$$

is negative when y is negative. Hence $-\frac{\partial}{\partial y} V(x, y)$ in the region $\{(x, y) | y \leq -2^{-4/3}\}$ is negative except at a maximum point. In particular, it is negative in the region $\{(x, y) | 0 \leq x \leq -\sqrt{3}y, y \leq -2^{-4/3}\}$ except at a maximum point. The rest of proof is similar to that of (iii) of example 12.

- (iv) It can be verified that the Gaussian curvature $K_{1/4}$ is everywhere zero except at the maximum points, where it has a singularity. Thus, from (9), $(E_c - V)\Delta V = -|\nabla V|^2$ everywhere. Since $V < E_c$ except at the maxima, we deduce that $\Delta V < 0$ except at the critical points of V (the maxima and the origin), and so K_E is everywhere negative when $E > 1/4$ except at the origin. Then the proof goes the same as that of (iv) of example 12.

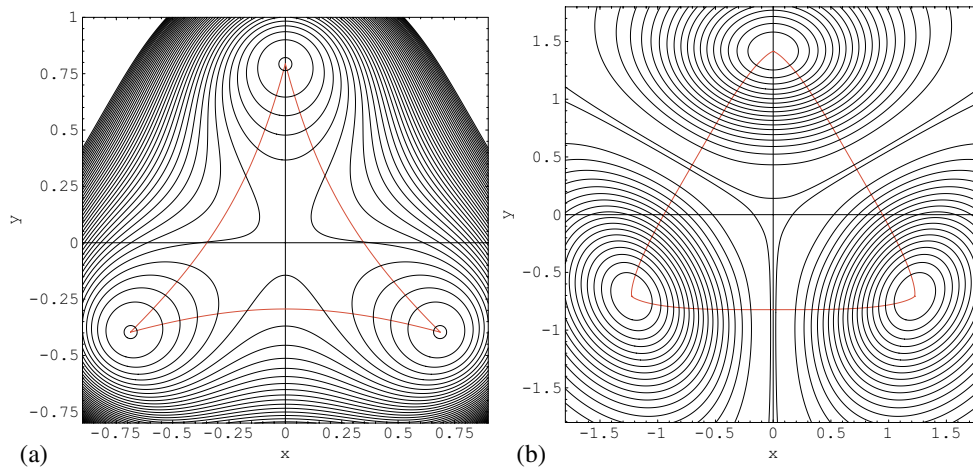


Figure 8. (a) Level sets of the potential V in example 14 and heteroclinics. (b) Level sets of the potential of form (2) and heteroclinics.

- (v) All trajectories can be obtained from straight lines in the complex w -plane.
- (vi) is a consequence of theorem 3. □

Remark 15. The logarithm of the absolute value of an analytic function is automatically harmonic, but it is easily checked explicitly, as follows. Write $\rho(z) = \rho(x + iy)$ as $\hat{\rho}(z, \bar{z})$. It is easy to verify that the Gaussian curvature

$$K(z) = \hat{K}(z, \bar{z}) = -\frac{\Delta \ln \hat{\rho}(z, \bar{z})}{\hat{\rho}^2(z, \bar{z})}$$

of any point other than z_1, z_2 and z_3 in the complex z -plane with the metric $\rho(z) |dz|$ is zero, since

$$\begin{aligned} \Delta \ln \hat{\rho}(z, \bar{z}) &= 4 \frac{\partial^2}{\partial z \partial \bar{z}} \ln \hat{\rho}(z, \bar{z}) \\ &= 2 \frac{\partial^2}{\partial z \partial \bar{z}} \left(\ln \left(\sqrt{2}z^3 + \frac{i}{\sqrt{2}} \right) + \ln \left(\sqrt{2}\bar{z}^3 - \frac{i}{\sqrt{2}} \right) \right) \\ &= 0. \end{aligned}$$

Remark 16. One thing we did not prove in examples 12 and 14 is that the set of bounded orbits for $E \in (E_c - \delta, E_c)$ is not more than the constructed subshift. This could probably be done with a bit more work, see [22].

Example 17. For the Lagrangian system with potential of form (1), there are 12 heteroclinic trajectories to the four maximum points $(\pm 1, \pm 1)$. They are given by straight lines $\{(x, y) \mid -1 \leq x \leq 1, y = \pm 1\}$, $\{(x, y) \mid x = \pm 1, -1 \leq y \leq 1\}$ and $\{(x, y) \mid -1 \leq x = \pm y \leq 1\}$, as in figure 4. All of them are non-degenerate.

Proof. Along the trajectory $(x_*(t), y_*(t))$ from $(-1, 1)$ to $(1, 1)$, the orthogonal component of the linearized Euler–Lagrange equation is

$$\frac{d^2}{dt^2}(\delta y) = 4x_*^2 e^{-(x_*^2+1)} \delta y.$$

The coefficient in the right hand side of the equality is positive except when x_* passes through zero. Thus there are no bounded solutions other than $\delta y = 0$.

For the trajectory $(x_*(t), y_*(t))$ from $(-1, 1)$ to $(1, -1)$, put $u = (x + y)/\sqrt{2}$, $v = (x - y)/\sqrt{2}$. Then $(u_*(t), v_*(t))$ is a trajectory from $(0, -\sqrt{2})$ to $(0, \sqrt{2})$ in the (u, v) -plane. The orthogonal component of the linearized Euler–Lagrange equation along $(u_*(t), v_*(t))$ is

$$\frac{d^2}{dt^2}(\delta v) = u_*^2 \left(1 + \frac{u_*^2}{2}\right) e^{-u_*^2} \delta v.$$

The coefficient on the right hand side is positive except when u_* passes through zero. Thus there are no bounded solutions other than zero. The non-degeneracy of all other heteroclinics follows from the symmetry of the system. □

4. Boundary value problem

This section is devoted to the dynamics of a particle moving in a small neighbourhood of a non-degenerate local maximum $O_e \in O_{\max}$ of the potential V . We choose the neighbourhood to be $U_e = U_{e,\delta}$ defined in (8). In this section all results are local, so we omit the subscript e in the rest of this section. As in [4, 9, 11, 12, 32], lemmata 18, 19, 20 and proposition 21 stated below characterize the main features of the dynamics. For the trajectories $\omega_x^\pm(t)$, let $z_x^\pm(t) \in W_{\text{loc}}^\pm$ be the corresponding orbits in the phase space.

Recall that for critical points of J (5), parametrized to achieve (7), J has the value

$$S = \int_a^b (L + E) dt,$$

where $[a, b]$ is the corresponding time-interval.

Proof. From the parametrization (7), $\sqrt{2(E - V)} = |\dot{\gamma}|$ so

$$\begin{aligned} J &= \int_a^b |\dot{\gamma}|^2 dt \\ &= \int_a^b \left(\left\{ \frac{1}{2} |\dot{\gamma}|^2 - V \right\} + \left\{ \frac{1}{2} |\dot{\gamma}|^2 + V \right\} \right) dt = S. \end{aligned} \quad \square$$

Lemma 18. *There exists $T > 0$ large, such that for any $x, y \in U$ and any $a < b \in \mathbb{R}$ with $b - a \geq T$, the Lagrangian system (3) has a unique trajectory $q(t)$ satisfying $q(a) = x$, $q(b) = y$, and $q(t) \in U$ for $a \leq t \leq b$. Furthermore,*

- if q is written as a function of (x, y, a, b, t) , then it is a C^2 function; in fact, it has the phase space representation

$$(q(t), p(t)) = z_x^+(t - a) + z_y^-(t - b) + \phi(x, y, a, b, t)e^{\mu_1(a-b)}, \quad (12)$$

where ϕ is a uniformly bounded C^2 function to $T^*\mathbb{R}^2 \cong \mathbb{R}^4$.

- the action

$$S(x, y, a, b) = \int_a^b (L(q(t), \dot{q}(t)) + E) dt$$

is C^2 and

$$S(x, y, a, b) = S^+(x) + S^-(y) + R(x, y, a, b)e^{\mu_1(a-b)} + (b - a)E,$$

where R is uniformly C^2 bounded as $b - a \rightarrow \infty$ and E , depending on x, y, a, b , is the energy of q .

The representation (12) indicates that $q(t) \rightarrow \omega_x^+(t-a)$ as $b \rightarrow \infty$, that $q(t) \rightarrow \omega_y^-(t-b)$ as $a \rightarrow -\infty$, and that $q(t) \rightarrow O$ as $a \rightarrow -\infty$ and $b \rightarrow \infty$, all uniformly on compact time intervals. Since the cotangent planes T_x^*U and T_y^*U intersect transversally the invariant manifolds W_{loc}^\pm of the hyperbolic equilibrium $(O, 0)$, lemma 18 is a consequence of lemma 19 below by putting $Y_v = T_x^*U$ and $Y_u = T_y^*U$. Lemma 19 can be derived from Shilnikov’s lemma [34] or from the strong λ -lemma [19].

Lemma 19. *Let g_t be the phase flow of the differential equation $\dot{z} = \mathcal{G}(z)$, where \mathcal{G} is a C^3 vector field on \mathbb{R}^n and $g_0 \equiv id$. Suppose that the origin 0 is a hyperbolic equilibrium with nonempty local stable and unstable manifolds W_{loc}^\pm , and that $\mu = \min |\operatorname{Re}(\operatorname{Spec} D\mathcal{G}(0))|$. Let Y_u and Y_v be C^2 manifolds intersecting transversally W_{loc}^- and W_{loc}^+ , respectively, at points z_u and z_v . Then for sufficiently large $T > 0$ and any $a < b$ with $b - a > T$, there exists a unique solution $z(t) = g_t(z(a))$ such that*

- $z(a) \in Y_v, z(b) \in Y_u,$
- *it has the representation*

$$z(t) = g_{t-a}(z_v) + g_{t-b}(z_u) + e^{\mu(a-b)}\phi(a, b, t), \tag{13}$$

where ϕ is a uniformly C^2 function to \mathbb{R}^n . If the manifolds Y_u and Y_v depend smoothly on a parameter taking values in a compact manifold, then ϕ is a uniformly bounded joint C^2 function with that parameter.

Proof. The proof follows closely that in [12]. Set $z = (u, v)$ and use coordinates $u \in W_{loc}^-$, $v \in W_{loc}^+$ in a neighbourhood $N = W_{loc}^- \times W_{loc}^+$ of the origin. Suppose Y_u is the graph of a function: $Y_u = \{(u, v) \mid u = f(v)\}$ and $g_t(Y_u) \cap N$ is given by $\{(u, v) \mid u = f_t(v)\}$. Then $z_u = f_0(0) = f(0)$. The strong λ -lemma [19] says that $\|f_t\|_{C^2} \leq Ce^{\mu t}$, $t \leq 0$, for some constant C . An analogous estimate $\|h_t\|_{C^2} \leq Ce^{-\mu t}$ also holds for $g_t(Y_v) \cap N = \{(u, v) \mid v = h_t(u)\}$ for $t \geq 0$, with $Y_v = \{(u, v) \mid v = h(u)\}$ and $z_v = h_0(0) = h(0)$. The boundary conditions require $z(t) = g_{t-a}(Y_v) \cap g_{t-b}(Y_u)$. Thus, any point on the set $\{z(t) \mid a \leq t \leq b\}$ satisfies $u = f_{t-b}(v)$ and $v = h_{t-a}(u)$. By the above estimates and the implicit function theorem, equation $v = h_{t-a}(f_{t-b}(v))$ has a unique solution $v(t) = g_{t-a}(z_v) + \eta(a, b, t)$ for $a \leq t \leq b$. The fact that

$$\begin{aligned} (0, v(t)) &= g_{t-a}(z_v) + (0, h_{t-a}(f_{t-b}(v))) - (0, h_{t-a}(0)) \\ &= g_{t-a}(z_v) + \Phi_{a,b,t}^+(v) \end{aligned}$$

gives $\|\Phi_{a,b,t}^+\|_{C^2} \leq C^2e^{\mu(a-b)}$ and $\Phi_{a,b,t}^+$ is quadratically small provided h_{t-a} and f_{t-b} are small: $\|\Phi_{a,b,t}^+\|_{C^2} \leq \|h_{t-a}\|_{C^2} \|f_{t-b}\|_{C^2}$. Hence $|\eta(a, b, t)| \leq C^2e^{\mu(a-b)}$. A similar inequality holds for the derivative of η in a, b, t . The representation (13) is proved for the coordinate v . The proof is similar for the coordinate u . When Y_u and Y_v depend on a parameter, the estimate above will be uniform in such a parameter. \square

Let

$$\zeta^+(x) := \lim_{t \rightarrow \infty} e^{\mu t} \dot{\omega}_x^+(t), \quad \zeta^-(y) := \lim_{t \rightarrow -\infty} e^{-\mu t} \dot{\omega}_y^-(t).$$

Lemma 20. *The energy $h(x, y, a, b)$ of the trajectory $q(t)$ is a C^2 function and has the form*

$$h(x, y, a, b) = e^{\mu_1(a-b)} (2\langle \zeta^+(x), \zeta^-(y) \rangle + h_1(x, y, a, b)),$$

where $h_1(x, y, a, b)$ converges to zero in the C^2 topology as $b - a \rightarrow \infty$.

Note that $\zeta^+(x)$ and $\zeta^-(y)$ are tangent vectors at O to the asymptotic trajectories ω_x^+ and ω_y^- , respectively. In other words, write

$$\zeta^+(x) = |\zeta^+(x)| \xi^+(x), \quad \zeta^-(y) = |\zeta^-(y)| \xi^-(y),$$

then

$$\xi^+(x) := \lim_{t \rightarrow \infty} \frac{\dot{\omega}_x^+(t)}{|\dot{\omega}_x^+(t)|}, \quad \text{and} \quad \xi^-(y) := \lim_{t \rightarrow -\infty} \frac{\dot{\omega}_y^-(t)}{|\dot{\omega}_y^-(t)|}.$$

For equal eigenvalues $\mu_1(O) = \mu_2(O)$, the scalar product $\langle \xi^+(x), \xi^-(y) \rangle$ may take any value in $[-1, 1]$ for a pair x and $y \in U$. When $\mu_1(O) \neq \mu_2(O)$, let $W_{\text{loc}}^{++} \subset W_{\text{loc}}^+$ and $W_{\text{loc}}^{--} \subset W_{\text{loc}}^-$ be one-dimensional local strong stable and unstable manifolds of the hyperbolic equilibrium $(O, 0) \in T^*\mathbb{R}^2$, namely the invariant manifolds tangent to the eigenvectors with eigenvalues $\pm\mu_2$ (the strong directions). The manifolds $W_{\text{loc}}^{\pm\pm}$ divide W_{loc}^{\pm} into connected components: $W_{\text{loc}}^+ \setminus W_{\text{loc}}^{++} = W_{\text{loc},R}^+ \cup W_{\text{loc},L}^+$, $W_{\text{loc}}^- \setminus W_{\text{loc}}^{--} = W_{\text{loc},R}^- \cup W_{\text{loc},L}^-$. The projections $\pi(W^{\pm\pm})$ to configuration space are identical and divide the neighbourhood U into connected components $U \setminus \pi(W_{\text{loc}}^{\pm\pm}) = U_R \cup U_L$.

When $\mu_1 \neq \mu_2$, we have $\langle \xi^+(x), \xi^-(y) \rangle \in \{0, \pm 1\}$. More precisely,

$$\langle \xi^+(x), \xi^-(y) \rangle = \begin{cases} -1 & \text{if } (x, y) \in (U_R \times U_R) \cup (U_L \times U_L) \\ +1 & \text{if } (x, y) \in (U_R \times U_L) \cup (U_L \times U_R). \end{cases}$$

Proof of lemma 20. Since we are concerned with the dynamics only in a neighbourhood U of O , we may shift and rotate coordinates if necessary so that the origin is located at O and in the new coordinates (we still use $x = (x_1, x_2) \in \mathbb{R}^2$ and conjugate momentum $p = (p_1, p_2) \in \mathbb{R}^2$) the Hessian matrix of V at O is diagonal and the Hamiltonian takes the form

$$H(x, p) = \frac{1}{2}|p|^2 - \frac{1}{2}v_1x_1^2 - \frac{1}{2}v_2x_2^2 + O_3(x), \tag{14}$$

where $-v_1, -v_2$ are the eigenvalues of the Hessian matrix of V at O . If $v_1 = v_2$ the result was proved in [9]. If $v_1 \neq v_2$, the eigenvalues of the Hamiltonian dynamics are $\pm\mu_1, \pm\mu_2$ with $\mu_1 = \sqrt{v_1}, \mu_2 = \sqrt{v_2}$. There exists a symplectic transformation $T : (x, p) \mapsto (u, v)$ given by

$$\begin{aligned} (x_1, x_2) &= T_1^{-1}(u, v) \\ &= \left(\frac{u_1 - \mu_1v_1}{\sqrt{2v_1}}, \frac{u_2 - \mu_2v_2}{\sqrt{2v_2}} \right) + O_2(u, v), \\ (p_1, p_2) &= T_2^{-1}(u, v) \\ &= \left(\frac{u_1 + \mu_1v_1}{\sqrt{2}}, \frac{u_2 + \mu_2v_2}{\sqrt{2}} \right) + O_2(u, v), \end{aligned}$$

such that $W_{\text{loc}}^+ = \{u = 0\}$, $W_{\text{loc}}^- = \{v = 0\}$, and the Hamiltonian takes the form

$$H(u, v) = \mu_1u_1v_1(1 + O(u, v)) + \mu_2u_2v_2(1 + O(u, v)). \tag{15}$$

If $\mu_1 < \mu_2$, then the coordinates can be chosen in such a way that $W_{\text{loc}}^{++} = \{u = 0, v_1 = 0\}$ and $W_{\text{loc}}^{--} = \{u_1 = 0, v = 0\}$. Hamilton's equations on W_{loc}^- have the form

$$\dot{u}_1 = \mu_1u_1 + O_2(u), \quad \dot{u}_2 = \mu_2u_2 + O_2(u), \tag{16}$$

where the right hand side of both equations is of class C^3 . By a C^2 change of variables $\eta = f_-(u) = (f_{1-}(u), f_{2-}(u))$, they can be transformed to linear equations $\dot{\eta}_1 = \mu_1\eta_1, \dot{\eta}_2 = \mu_2\eta_2$ unless $\mu_2 = 2\mu_1$ [35].

Hence if $\mu_2 \neq 2\mu_1$ the phase flow on W_{loc}^- takes the form

$$\begin{aligned} g_t(u, 0) &= (f_-^{-1}(e^{\mu_1 t} f_{1-}(u), e^{\mu_2 t} f_{2-}(u)), 0) \\ &= (e^{\mu_1 t}((f_{1-}(u), e^{(\mu_2 - \mu_1)t} f_{2-}(u)) + G_-(u, t)), 0) \end{aligned} \tag{17}$$

where $G_- = (G_{1-}, G_{2-})$ with $\|G_-\|_{C^2} \rightarrow 0$ uniformly on W_{loc}^- as $t \rightarrow -\infty$. Note that

$$\begin{aligned} f_{1-}(u) = 0 & \quad \text{and} \quad G_{1-}(u, t) = 0 & \quad \text{if } u_1 = 0, \\ f_{2-}(u) = 0 & \quad \text{and} \quad G_{2-}(u, t) = 0 & \quad \text{if } u_2 = 0. \end{aligned} \tag{18}$$

The representation given in (17) is called an exponential expansion in [19]. A similar representation holds for the flow on W_{loc}^+ :

$$g_t(0, v) = (0, e^{-\mu_1 t}((f_{1+}(v), e^{-(\mu_2 - \mu_1)t} f_{2+}(v)) + G_+(v, t))) \tag{19}$$

where $G_+ = (G_{1+}, G_{2+})$ with $\|G_+\|_{C^2} \rightarrow 0$ uniformly on W_{loc}^+ as $t \rightarrow \infty$. Note also that

$$\begin{aligned} f_{1+}(v) = 0 & \quad \text{and} \quad G_{1+}(v, t) = 0 & \quad \text{if } v_1 = 0, \\ f_{2+}(v) = 0 & \quad \text{and} \quad G_{2+}(v, t) = 0 & \quad \text{if } v_2 = 0. \end{aligned} \tag{20}$$

Moreover,

$$\lim_{t \rightarrow -\infty} e^{-\mu_1 t} g_t(u, 0) = (f_{1-}(u), \lim_{t \rightarrow -\infty} e^{(\mu_2 - \mu_1)t} f_{2-}(u), 0, 0), \tag{21}$$

$$\lim_{t \rightarrow \infty} e^{\mu_1 t} g_t(0, v) = (0, 0, f_{1+}(v), \lim_{t \rightarrow \infty} e^{-(\mu_2 - \mu_1)t} f_{2+}(v)). \tag{22}$$

Put $t = (a + b)/2$ in (12), by (17) and (19),

$$\begin{aligned} \left(q \left(\frac{a+b}{2} \right), p \left(\frac{a+b}{2} \right) \right) &= e^{\mu_1(a-b)/2} (f_{1-}(u), e^{(\mu_2 - \mu_1)(a-b)/2} f_{2-}(u), \\ & \quad f_{1+}(v), e^{(\mu_2 - \mu_1)(a-b)/2} f_{2+}(v)) \\ & \quad + e^{\mu_1(a-b)/2} F(u, v, a, b), \end{aligned} \tag{23}$$

where $u = u(b)$, $v = v(a)$ and $\|F\|_{C^2} \rightarrow 0$ as $b - a \rightarrow \infty$. (Note that $u \neq 0$ and $v \neq 0$ for any finite a and b .) Substituting (23) into (15), we get an estimate of the energy at $q((a+b)/2)$:

$$\begin{aligned} h(x, y, a, b) &= e^{\mu_1(a-b)} (\mu_1 f_{1-}(u) f_{1+}(v) + \mu_2 e^{(\mu_2 - \mu_1)(a-b)} f_{2-}(u) f_{2+}(v) + h_2) \\ &= \begin{cases} e^{\mu_1(a-b)} (\mu_1 f_{1-}(u) f_{1+}(v) + \mu_1 f_{2-}(u) f_{2+}(v) + h_2) & \text{if } \mu_1 = \mu_2 \\ e^{\mu_1(a-b)} (\mu_1 f_{1-}(u) f_{1+}(v) + h_3) & \text{if } \mu_1 < \mu_2, \end{cases} \end{aligned} \tag{24}$$

where $h_2 = h_2(x, y, a, b)$ and $h_3 = h_3(x, y, a, b)$ satisfying $\|h_2\|_{C^2} \rightarrow 0$ and $\|h_3\|_{C^2} \rightarrow 0$ as $b - a \rightarrow \infty$. Passing to the variables x, p and using (21) and (22), we get

$$\lim_{t \rightarrow \infty} e^{\mu_1 t} \dot{\omega}_x^+(t) = \frac{\mu_1}{\sqrt{2}} (f_{1+}(v), \frac{\mu_2}{\mu_1} \lim_{t \rightarrow \infty} e^{-(\mu_2 - \mu_1)t} f_{2+}(v)), \tag{25}$$

$$\lim_{t \rightarrow -\infty} e^{-\mu_1 t} \dot{\omega}_y^-(t) = \frac{1}{\sqrt{2}} (f_{1-}(u), \lim_{t \rightarrow -\infty} e^{(\mu_2 - \mu_1)t} f_{2-}(u)). \tag{26}$$

Putting together (24)–(26), we obtain the desired result:

$$h(x, y, a, b) = e^{\mu_1(a-b)} (2 \langle \lim_{t \rightarrow \infty} e^{\mu_1 t} \dot{\omega}_x^+(t), \lim_{t \rightarrow -\infty} e^{-\mu_1 t} \dot{\omega}_y^-(t) \rangle + h_1),$$

where $h_1 = h_1(x, y, a, b)$ equals h_2 if $\mu_1 = \mu_2$ or h_3 if $\mu_1 < \mu_2$.

If $\mu_2 = 2\mu_1$ one can linearize just the first equation of (16) as in [11], and achieve the same result. In fact this argument works for any $\mu_2 > \mu_1$. □

Take small $\nu > 0$ and let

$$\begin{aligned} B^- &= \{(x, y) \in U^2 \mid \langle \zeta^+(x), \zeta^-(y) \rangle \leq -\nu\}, \\ B^+ &= \{(x, y) \in U^2 \mid \langle \zeta^+(x), \zeta^-(y) \rangle \geq \nu\}. \end{aligned}$$

Then for $(x, y) \in B^-$ or B^+ the function $h(x, y, a, b)$ is monotone in $a - b$ (for $b - a$ sufficiently large). Thus, solving the equation $h(x, y, a, b) = \epsilon$ for small ϵ yields a function $\tau_\epsilon(x, y)$, with $b - a = \tau_\epsilon$. This together with lemmata 18 and 20 gives the following result.

Proposition 21. *There exists $\epsilon_0 < 0$ (respectively, $\epsilon_1 > 0$) such that for all $\epsilon \in (\epsilon_0, 0)$ (respectively, $\epsilon \in (0, \epsilon_1)$):*

- for any $(x, y) \in B^-$ (respectively, B^+), there exists a unique trajectory $q_{x,y}^\epsilon : [a, b] \rightarrow U$ of energy ϵ connecting points x and y , with $q_{x,y}^\epsilon(a) = x$, $q_{x,y}^\epsilon(b) = y$, and $b - a = \tau$.
- $\tau = \tau_\epsilon(x, y)$ is a C^2 function on B^- (respectively, B^+) and

$$\tau_\epsilon(x, y) = -\frac{\log |\epsilon|}{\mu_1} + \mu(x, y, \epsilon),$$

where the function μ is uniformly bounded on B^- (respectively, B^+) as $\epsilon \rightarrow 0$.

- we have

$$(q_{x,y}^\epsilon(t), p_{x,y}^\epsilon(t)) = z_x^+(t - a) + z_y^-(t - b) + \epsilon \zeta(x, y, \epsilon),$$

where the function ζ is uniformly C^1 bounded as $\epsilon \rightarrow 0$.

- the action $S(x, y, a, b)$ of the trajectory $q_{x,y}^\epsilon$ regarded as a function of (x, y) is C^2 on B^- (respectively, B^+) and

$$S(x, y, a, b) = S^+(x) + S^-(y) + \epsilon r(x, y, \epsilon) - \epsilon \log |\epsilon| / \mu_1, \tag{27}$$

where r is uniformly C^2 bounded on B^- (respectively, B^+) as $\epsilon \rightarrow 0$.

Remark 22. When $\mu_1 = \mu_2$, a pair of points x and y is contained in B^- or B^+ if x and y are sufficiently bounded away from the maximum point O and if $\langle \xi^+(x), \xi^-(y) \rangle$ is sufficiently bounded away from zero. When $\mu_1 < \mu_2$, an additional condition is needed to guarantee that (x, y) is in B^- or B^+ . The condition is that x must be sufficiently bounded away from $\pi(W_{loc}^{++})$ and y must be sufficiently bounded away from $\pi(W_{loc}^{--})$. This can be seen from (18), (20), (25) and (26). As a matter of fact, $f_{1-}(u)$ takes the form $f_{1-}(u) = u_1 \tilde{f}_{1-}(u)$, with $\tilde{f}_{1-}(0) \neq 0$ [11, 12, 19, 35]. Similarly, $f_{1+}(v) = v_1 \tilde{f}_{1+}(v)$, with $\tilde{f}_{1+}(0) \neq 0$. This remark explains the definition of the admissibility condition in definition 1.

5. Shadowing hetero/homoclinic trajectories

The boundaries $\partial U_{e,\delta}$ of $U_{e,\delta}$ are C^2 .

Suppose that $\Gamma_{i-1,i} = \Gamma_{k_i}$, $k_i \in K$, is a hetero/homoclinic trajectory such that $\Gamma_{i-1,i}(0) = y_{i-1}^\dagger \in \partial U_{e_{i-1}}$ and $\Gamma_{i-1,i}(T_0) = x_i^\dagger \in \partial U_{e_i}$ for some $T_0 = T_0(y_{i-1}^\dagger, x_i^\dagger) > 0$. See figure 9. Let W_k be a small neighbourhood of $\Gamma_k((-\infty, \infty))$. By our assumption, the points y_{i-1}^\dagger and x_i^\dagger are not conjugate to each other on the fixed energy level $\{E = 0\}$. Then by the implicit function theorem, there are neighbourhoods $\Delta_{y_{i-1}}$ of y_{i-1}^\dagger in $\partial U_{e_{i-1}}$, Δ_{x_i} of x_i^\dagger in ∂U_{e_i} , and there are $\epsilon_0 < 0 < \epsilon_1$ such that for all $\epsilon_0 < \epsilon < \epsilon_1$ any points y_{i-1} in $\Delta_{y_{i-1}} \subset \partial U_{e_{i-1}}$ and x_i in $\Delta_{x_i} \subset \partial U_{e_i}$ can be connected by a unique trajectory $q_{i-1,i} : [0, T_\epsilon] \rightarrow W_{k_i}$ of energy ϵ satisfying $q_{i-1,i}(0) = y_{i-1}$ and $q_{i-1,i}(T_\epsilon) = x_i$ for some $T_\epsilon = T_\epsilon(y_{i-1}, x_i) > 0$. If $q_{i-1,i}$ and T_ϵ are regarded as functions of (y_{i-1}, x_i, ϵ) , then they depend C^2 on their variables.

Theorem 23. *There exists $\epsilon_0 < 0$ (respectively, $\epsilon_1 > 0$) such that for any $\epsilon_0 < \epsilon < 0$ (respectively, $0 < \epsilon < \epsilon_1$) and any sequence of hetero/homoclinic trajectories $\{\Gamma_{k_i}\}_{i \in \mathbb{Z}}$ admissible for $E < 0$ (respectively, $E > 0$) the system admits a unique (up to time shift) trajectory $\Upsilon : \mathbb{R} \rightarrow M_\epsilon \cap (\bigcup_{k \in K} W_k)$ of energy ϵ and a sequence $\dots < a_{-1} < b_{-1} < a_0 < b_0 < \dots$ such that for all $i \in \mathbb{Z}$*

- $\Upsilon([b_{i-1}, a_i]) \subset W_{k_i}$, $\Upsilon(b_{i-1}) \in \Delta_{y_{i-1}}$, $\Upsilon(a_i) \in \Delta_{x_i}$, and $\Upsilon([a_i, b_i]) \subset U_{e_i}$.

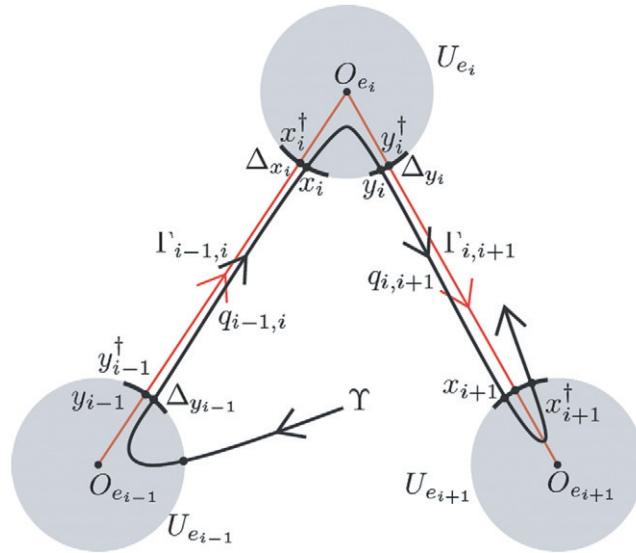


Figure 9. Decomposition of paths into segments inside neighbourhoods of the maxima and segments between them.

More precisely,

- $a_i - b_{i-1} = T_\epsilon(\Upsilon(b_{i-1}), \Upsilon(a_i))$,
- $\Upsilon(t) = q_{i-1,i}(t - b_{i-1})$ for $b_{i-1} \leq t \leq a_i$,
- $\Upsilon(t) = q_{\Upsilon(a_i), \Upsilon(b_i)}^\epsilon(t)$ for $a_i \leq t \leq b_i$, with $b_i - a_i = \tau_\epsilon(\Upsilon(a_i), \Upsilon(b_i))$.

As $\epsilon \rightarrow 0$, $\Upsilon(b_{i-1}) \rightarrow y_{i-1}^\dagger$, $\Upsilon(a_i) \rightarrow x_i^\dagger$, and $a_i - b_{i-1} \rightarrow T_0(y_{i-1}^\dagger, x_i^\dagger)$.

Theorem 23 implies that there is an invariant set Λ_ϵ on the energy level $\{E = \epsilon\}$ on which the system is a suspension of the topological Markov chain G_K^- or G_K^+ (i.e. theorems 5 and 6).

To this end, we shall obtain a more detailed result first. We take the cross section $N \in T\mathbb{R}^2$ described in theorem 5 to be the annuli whose projection to the configuration space is $\bigcup_{O_e \in O_{\max}} \partial U_e$. That is, we require that if $(x, v) \in N$ then x belongs to some ∂U_e , $|v| = \sqrt{2(\epsilon - V(x))}$, and the inner product of the velocity vector with the inner normal of ∂U_e is positive. The Lagrangian flow induces a map (the Poincaré map) \mathcal{P}_ϵ on a subset of N :

$$\mathcal{P}_\epsilon : (x_i, v_i) \mapsto (x_{i+1}, v_{i+1}). \tag{28}$$

The meaning of \mathcal{P}_ϵ is that if x_i, v_i are the position and velocity with which a particle enters $\bigcup_{O_e \in O_{\max}} U_e$ then x_{i+1}, v_{i+1} are the next position and velocity with which it enters $\bigcup_{O_e \in O_{\max}} U_e$.

Suppose the corresponding orbits of the hetero/homoclinic trajectories $\{\Gamma_k\}_{k \in K}$ in the phase space $T\mathbb{R}^2$ intersect N at a set \mathcal{A}_0 :

$$\mathcal{A}_0 = \{(x^{(k)}, v^{(k)})\}_{k \in K}. \tag{29}$$

(We can take all U_e sufficiently small so that N and $(\Gamma_k, \dot{\Gamma}_k)$ intersect at only one point for each k .) Define two topological Markov chains $\Sigma_{\mathcal{A}_0}^-$ and $\Sigma_{\mathcal{A}_0}^+$, which are respectively topologically conjugate to the subshift with graphs G_K^- and G_K^+ , by

$$\begin{aligned} \Sigma_{\mathcal{A}_0}^\pm &:= \{(x_i^\dagger, v_i^\dagger)\}_{i \in \mathbb{Z}} \mid (x_i^\dagger, v_i^\dagger) = (x^{(k_i)}, v^{(k_i)}), k_i \in K, \\ k_i &\mapsto k_{i+1} \text{ complying with the graph } G_K^- \text{ or } G_K^+ \text{ for all } i \in \mathbb{Z}. \end{aligned} \tag{30}$$

Let \mathcal{P}_0^\pm be the subshift $\Sigma_{\mathcal{A}_0}^\pm \rightarrow \Sigma_{\mathcal{A}_0}^\pm$,

$$(x_i^\dagger, v_i^\dagger) \mapsto (x_{i+1}^\dagger, v_{i+1}^\dagger). \tag{31}$$

Proposition 24. *Let the sequence $\{(x_i^\dagger, v_i^\dagger) \in \mathcal{A}_0\}_{i \in \mathbb{Z}}$ be an orbit of the map \mathcal{P}_0^- (respectively, \mathcal{P}_0^+). Then there are $\epsilon_0 < 0 < \epsilon_1$ so that for any $\epsilon \in (\epsilon_0, 0)$ (respectively, $(0, \epsilon_1)$) there exists a unique sequence $\{(x_i^*(\epsilon), v_i^*(\epsilon))\}_{i \in \mathbb{Z}}$ which is a hyperbolic orbit of the map \mathcal{P}_ϵ such that for every i , $(x_i^*(\epsilon), v_i^*(\epsilon))$ is C^1 in ϵ , uniformly in i , and $x_i^*(\epsilon) \in \Delta_{x_i}$, $\lim_{\epsilon \rightarrow 0} x_i^*(\epsilon) = x_i^\dagger$, $\lim_{\epsilon \rightarrow 0} v_i^*(\epsilon) = v_i^\dagger$.*

Define the following action function on $\Delta_{y_{i-1}} \times \Delta_{x_i}$:

$$S_\epsilon(y_{i-1}, x_i) := \int_0^{T_\epsilon(y_{i-1}, x_i)} (L(q_{i-1,i}(t), \dot{q}_{i-1,i}(t)) + \epsilon) dt.$$

The function S_ϵ is jointly C^2 in (y_{i-1}, x_i) and ϵ , and satisfies

$$dS_\epsilon(y_{i-1}, x_i) = -\langle p_{y_{i-1}}^+, dy_{i-1} \rangle + \langle p_{x_i}^-, dx_i \rangle$$

with $p_{y_{i-1}}^+ := v_{y_{i-1}}^+ := \dot{q}_{i-1,i}(0)$, $p_{x_i}^- := v_{x_i}^- := \dot{q}_{i-1,i}(T_\epsilon)$.

We denote the sequence $\{(y_{i-1}^\dagger, x_i^\dagger)\}_{i \in \mathbb{Z}}$ determined by an AI-trajectory by $\{z_i^\dagger\}_{i \in \mathbb{Z}} = z^\dagger \in Z$, where

$$Z := \prod_{i \in \mathbb{Z}} (\Delta_{y_{i-1}} \times \Delta_{x_i}),$$

is an open set of $\prod_{i \in \mathbb{Z}} (\partial U_{e_{i-1}} \times \partial U_{e_i})$ endowed with the supremum norm. The Jacobi length of a concatenation is the formal sum

$$\sum_{i \in \mathbb{Z}} S_\epsilon(y_{i-1}, x_i) + S(x_i, y_i, 0, \tau_\epsilon(x_i, y_i)).$$

Rewrite this (which does not change the critical points) by adding and subtracting $\sum_{i \in \mathbb{Z}} S^+(x_i) + S^-(y_i)$ and subtracting the constant term $\sum_{i \in \mathbb{Z}} -\frac{\epsilon \log|\epsilon|}{\mu_1(O_{e_i})}$, to obtain, using (27), the formal functional

$$W(z, \epsilon) = \sum_i w_\epsilon(y_{i-1}, x_i) + \epsilon r(x_i, y_i, \epsilon)$$

with

$$w_\epsilon(y_{i-1}, x_i) = S^-(y_{i-1}) + S_\epsilon(y_{i-1}, x_i) + S^+(x_i).$$

Note that since $x_i \in \partial U_{e_i}$ then $S^+(x_i) = \delta$, and similarly $S^-(y_i) = \delta$, but we write h_ϵ more generally in case one might prefer to take different curves around O_{e_i} from ∂U_{e_i} . Further, we define a map

$$F : Z \times \mathbb{R} \rightarrow l_\infty, \\ (z, \epsilon) \mapsto \{F_i(z, \epsilon)\}_{i \in \mathbb{Z}},$$

where l_∞ is the subspace of $(\mathbb{R}^2 \times \mathbb{R}^2)^\mathbb{Z}$ with bounded supremum norm and $F_i = D_{z_i} W$. (Remark: although the value of W may be infinite due to the summation over all $i \in \mathbb{Z}$, the definition of F_i makes sense because the derivative is taken with respect to z_i (not with respect to z) and there are only finitely many terms having variable z_i in the summation.) It is not difficult to see that F is a C^1 function. By our construction, z^\dagger is the only solution for $F(z, 0) = 0$ and corresponds to an admissible sequence of hetero/homoclinic trajectories (i.e. an AI-trajectory) associated with z^\dagger .

Proposition 25. For slightly negative or positive ϵ , a point $z^*(\epsilon) = z^* = \{(y_{i-1}^*, x_i^*)\}_{i \in \mathbb{Z}}$ which is a zero of $F(\cdot, \epsilon)$ corresponds to a trajectory Υ of energy ϵ .

Proof. This is Maupertuis's principle. It can be checked by differentiation. \square

Lemma 26. For each $i \in \mathbb{Z}$, the function $F_i(\cdot, 0)$ on $\Delta_{y_{i-1}} \times \Delta_{x_i}$ has a non-degenerate zero at $z_i^\dagger = (y_{i-1}^\dagger, x_i^\dagger)$.

Proof. $F_i((y_{i-1}, x_i), 0)$ is the derivative of the sum of actions

$$w_0(y_{i-1}, x_i) = S^-(y_{i-1}) + S_0(y_{i-1}, x_i) + S^+(x_i)$$

which is the Jacobi length from $O_{e_{i-1}}$ to O_{e_i} via the points y_{i-1}, x_i . In addition, $\Gamma_{i-1,i} (\equiv \Gamma_{k_i})$ is the concatenation $\omega_{y_{i-1}}^- \cdot q_{y_{i-1}, x_i} \cdot \omega_{x_i}^+$. Hence a zero of $F_i(\cdot, 0)$ is a critical point of the action functional that is restricted to a finite-dimensional submanifold consisting of broken trajectories with break points y_{i-1} and x_i connecting $O_{e_{i-1}}$ to O_{e_i} . Thus, the lemma follows from the assumption that $\Gamma_{i-1,i}$ is a non-degenerate hetero/homoclinic trajectory. \square

Proof of theorem 23. Theorem 23 is a consequence of proposition 25 and lemma 26. The sequence of hetero/homoclinic trajectories $\{\Gamma_{k_i}\}_{i \in \mathbb{Z}}$ corresponds to a non-degenerate zero of $F(\cdot, 0)$ and the implicit function theorem gives rise to a locally unique continuation provided $\epsilon_0 < \epsilon < \epsilon_1$ for some $\epsilon_0 < 0 < \epsilon_1$. The values of ϵ_0 and ϵ_1 can be chosen independent of the sequence $\{\Gamma_{k_i}\}_{i \in \mathbb{Z}}$ because $k_i \in K$ and K is a finite set. \square

Proof of proposition 24. The sequence $\{(x_i^\dagger, v_i^\dagger)\}_{i \in \mathbb{Z}}$ corresponds to a unique sequence $z^\dagger = \{(y_{i-1}^\dagger, x_i^\dagger)\}_{i \in \mathbb{Z}}$, which is a simple zero of $F(\cdot, 0)$. Therefore, there is a C^1 -function $z^*(\epsilon) = \{z_i^*(\epsilon)\}_{i \in \mathbb{Z}} = \{(y_{i-1}^*(\epsilon), x_i^*(\epsilon))\}_{i \in \mathbb{Z}}$ in the space Z such that $F(z^*(\epsilon), \epsilon) = 0$ if $\epsilon_0 < \epsilon < \epsilon_1$ for some $\epsilon_0 < 0 < \epsilon_1$ by lemma 26 and the implicit function theorem. For each integer i , the point $((y_{i-1}^*(\epsilon), x_i^*(\epsilon)))$ corresponds C^1 -diffeomorphic to $(x_i^*(\epsilon), v_i^*(\epsilon))$. The hyperbolicity follows from the uniform hyperbolicity of the set \mathcal{A}_ϵ in theorems 5 and 6. \square

Proof of theorems 5 and 6. The set $\Sigma_{\mathcal{A}_0}$ with the product topology is a Cantor set as soon as the corresponding graph is non-trivial (communicating with at least one branch point). The mapping composed of the following mappings

$$\prod_{i \in \mathbb{Z}} (x_i^\dagger, v_i^\dagger) \xrightarrow{f_1} \prod_{i \in \mathbb{Z}} (y_{i-1}^\dagger, x_i^\dagger) \xrightarrow{\Phi_\epsilon} \prod_{i \in \mathbb{Z}} (y_{i-1}^*(\epsilon), x_i^*(\epsilon)) \xrightarrow{f_2} \prod_{i \in \mathbb{Z}} (x_i^*(\epsilon), v_i^*(\epsilon))$$

is continuous in the product topologies because f_1 , Φ_ϵ and f_2 are all continuous (see, for example [16]). The projection $\prod_{i \in \mathbb{Z}} (x_i^*(\epsilon), v_i^*(\epsilon)) \xrightarrow{\pi} (x_0^*(\epsilon), v_0^*(\epsilon))$ is also continuous. Let $g_\epsilon := \pi \circ f_2 \circ \Phi_\epsilon \circ f_1$. Thence the two sets

$$g_\epsilon(\Sigma_{\mathcal{A}_0}) := \mathcal{A}_\epsilon$$

and $\Sigma_{\mathcal{A}_0}$ with the product topologies are homeomorphic to each other because all f_1 , Φ_ϵ , f_2 and π are injective. The homeomorphism g_ϵ^{-1} is then the desired conjugacy: because

$g_\epsilon \circ \mathcal{P}_0(\{(x_i^\dagger, v_i^\dagger)\}_{i \in \mathbb{Z}}) = (x_1^*(\epsilon), v_1^*(\epsilon))$ by the time translation invariance of the system, the following diagram is commutative

$$\begin{CD} \Sigma_{\mathcal{A}_0} \ni \{(x_i^\dagger, v_i^\dagger)\}_{i \in \mathbb{Z}} @>\mathcal{P}_0>> \{(x_{i+1}^\dagger, v_{i+1}^\dagger)\}_{i \in \mathbb{Z}} \in \Sigma_{\mathcal{A}_0} \\ @Vg_\epsilon VV @VVg_\epsilon V \\ \mathcal{A}_\epsilon \ni (x_0^*(\epsilon), v_0^*(\epsilon)) @>\mathcal{P}_\epsilon>> (x_1^*(\epsilon), v_1^*(\epsilon)) \in \mathcal{A}_\epsilon. \end{CD}$$

The proof of uniform hyperbolicity and the estimate of Lyapunov exponents are in a similar manner to that of [10]. We were able to define $W(\cdot, \epsilon)$ because any $x_i \in \Delta_{x_i}$ can be connected to any $y_i \in \Delta_{y_i}$ by a unique (up to time shift) trajectory of energy ϵ provided that the time needed to travel from x_i to y_i is sufficiently long, also any $y_i \in \Delta_{y_i}$ can be connected to any $x_{i+1} \in \Delta_{x_{i+1}}$ by a unique (up to time shift) trajectory of energy ϵ provided the trajectory is near $\Gamma_{i, i+1}$. Actually, given a pair $x_i \in \Delta_{x_i}$ and $x_{i+1} \in \Delta_{x_{i+1}}$, it determines a unique (up to time shift) trajectory of energy ϵ connecting them by gluing the aforementioned two unique trajectories because the aforementioned y_i can be determined uniquely by x_i and x_{i+1} and the resulting trajectory has no velocity discontinuity at y_i . Indeed, our non-degeneracy condition implies that x_{i+1} is not conjugate to O_{e_i} , therefore

$$\det D_{y_i}^2(w_0(y_i, x_{i+1})) \neq 0.$$

Then for small ϵ we can locally solve the equation

$$D_{y_i}(w_\epsilon(y_i, x_{i+1}) + \epsilon r(x_i, y_i, \epsilon)) = 0$$

for

$$y_i = \chi(x_i, x_{i+1}, \epsilon).$$

So we can define

$$\bar{S}_\epsilon(x_i, x_{i+1}) := w_\epsilon(\chi(x_i, x_{i+1}, \epsilon), x_{i+1}) + \epsilon r(x_i, \chi(x_i, x_{i+1}, \epsilon), \epsilon).$$

Therefore, we reduce $W(\cdot, \epsilon)$ to a functional Φ_ϵ of the sequence $x = \{x_i\}_{i \in \mathbb{Z}}$ only,

$$\Phi_\epsilon(x) := \sum_{i \in \mathbb{Z}} \bar{S}_\epsilon(x_i, x_{i+1}).$$

Critical points of Φ_ϵ correspond to orbits of the symplectic map with the generating function $\bar{S}_\epsilon(x_i, x_{i+1})$. It was proved by Aubry *et al* [2] that if the generating function has non-degenerate mixed second derivative (i.e. the twist condition) then the non-degeneracy of a critical point of Φ_ϵ is equivalent to uniform hyperbolicity of the corresponding orbit of the associated symplectic twist map.

The Poincaré map $\mathcal{P}_\epsilon : (x_i, v_i) \mapsto (x_{i+1}, v_{i+1})$ defined in (28) is C^2 , and can be generated by

$$D_{x_{i+1}} \bar{S}_\epsilon(x_i, x_{i+1}) = v_{i+1}, \quad D_{x_i} \bar{S}_\epsilon(x_i, x_{i+1}) = -v_i.$$

Consequently, non-degeneracy of $D_{x_i x_{i+1}}^2 \bar{S}_\epsilon(x_i, x_{i+1})$ is equivalent to boundedness of the derivative of \mathcal{P}_ϵ :

$$\|(D_{x_i x_{i+1}}^2 \bar{S}_\epsilon(x_i, x_{i+1}))^{-1}\| \leq C \epsilon^{-1} \iff \|D\mathcal{P}_\epsilon(x_i, v_i)\| \leq c \epsilon^{-1}$$

for some constants C and c .

Proposition 21 implies that the time $\tilde{\tau}_\epsilon$ needed to connect x_i and x_{i+1} is of order $\log |\epsilon|^{-1}$, the Poincaré map \mathcal{P}_ϵ , as a time- $\tilde{\tau}_\epsilon$ map induced from the Lagrangian flow, is thus uniformly C^1 bounded by $c|\epsilon|^{-1}$, where $\tilde{\tau}_\epsilon = \tau_\epsilon(x_i, \chi(x_i, x_{i+1}, \epsilon)) + T_\epsilon(\chi(x_i, x_{i+1}, \epsilon), x_{i+1})$. This gives an upper bound of the Lyapunov exponents. A lower bound of this order comes from the proof of proposition 1 of [2]. Note that the Lyapunov exponents of orbits of the topological Markov chain depend on the eigenvalues at the maxima, and the angles turned there if circular. \square

Acknowledgments

Chen is partially supported by NSC 99-2115-M-001-007, NSC 100-2115-M-001-007, NSC 101-2115-M-001-010 and 2010-2011 France-Taiwan Orchid Joint Project Programme. He thanks the Université de Provence and the University of Warwick for their hospitality during his visits (the latter was funded by EPSRC grant EP/G021163/1), and thanks Massimiliano Berti and Philippe Bolle for discussions.

References

- [1] Aubry S and Abramovici G 1990 Chaotic trajectories in the standard map: the concept of anti-integrability *Physica D* **43** 199–219
- [2] Aubry S, MacKay R S and Baesens C 1992 Equivalence of uniform hyperbolicity for symplectic twist maps and phonon gap for Frenkel–Kontorova models *Physica D* **56** 123–34
- [3] Berti M and Bolle P 1998 Variational construction of homoclinics and chaos in presence of a saddle–saddle equilibrium *Ann. Scuola Norm. Sup. Pisa Cl. Sci.* **27** 331–77 (<https://eudml.org/doc/84361>)
- [4] Bertotti M L and Bolotin S V 2003 Chaotic trajectories for natural systems on a torus *Discrete Contin. Dyn. Syst.* **9** 1343–57
- [5] Birkhoff G D 1927 *Dynamical Systems (AMS Colloquium Publications vol 9)* (Providence, RI: American Mathematical Society) p 39
Birkhoff G D 1917 Dynamical systems with two degrees of freedom *Trans. Am. Math. Soc.* **18** 199–300
- [6] Bleher S, Grebogi C and Ott E 1990 Bifurcation to chaotic scattering *Physica D* **46** 87–121
- [7] Bleher S, Ott E and Grebogi C 1989 Route to chaotic scattering *Phys. Rev. Lett.* **63** 919–22
- [8] Bolotin S V 1978 Libration motions of natural dynamical systems *Vestn. Mosk. Univ. Ser. I* **6** 72–7
- [9] Bolotin S V and MacKay R S 2000 Periodic and chaotic trajectories of the second species for the n -centre problem *Celest. Mech. Dyn. Astron.* **77** 49–75
- [10] Bolotin S V and MacKay R S 2006 Nonplanar second species periodic and chaotic trajectories for the circular restricted three-body problem *Celest. Mech. Dyn. Astron.* **94** 433–49
- [11] Bolotin S V and Rabinowitz P H 1998 A variational construction of chaotic trajectories for a reversible Hamiltonian system *J. Diff. Eqns* **148** 364–87
- [12] Bolotin S V and Rabinowitz P H 1998 A variational construction of chaotic trajectories for a Hamiltonian system on a torus *Boll. Unione Mat. Ital. Sez. B* **1** 541–70 (<https://eudml.org/doc/195529>)
- [13] Buffoni B and Séré E 1996 A global condition for quasi-random behavior in a class of conservative systems *Commun. Pure Appl. Math.* **49** 285–305
- [14] Buttazzo G, Giaquinta M and Hildebrandt S 1998 *One-dimensional Variational Problems—An Introduction* (New York: Clarendon Press/Oxford University Press)
- [15] Chen Y-C 2004 Anti-integrability in scattering billiards *Dyn. Syst.* **19** 145–59
- [16] Chen Y-C 2005 Bernoulli shift for second order recurrence relations near the anti-integrable limit *Discrete Contin. Dyn. Syst. B* **5** 587–98
- [17] Chen Y-C 2010 On topological entropy of billiard tables with small inner scatterers *Adv. Math.* **224** 432–60
- [18] Churchill R C and Rod D L 1976 Pathology in dynamical systems. II. Applications *J. Diff. Eqns* **21** 66–112
- [19] Deng B 1989 The Sil’nikov problem, exponential expansion, strong λ -lemma, C^1 -linearization, and Homoclinic Bifurcation *J. Diff. Eqns* **79** 189–231
- [20] Devaney R L 1976 Homoclinic orbits in Hamiltonian systems *J. Diff. Eqns* **21** 431–8
- [21] Devaney R L 1978 Transversal homoclinic orbits in an integrable system *Am. J. Math.* **100** 631–42
- [22] Devaney R L and Nitecki Z 1979 Shift automorphisms in the Hénon mapping *Commun. Math. Phys.* **67** 137–46
- [23] Ding M 1992 Topological-entropy and bifurcations of chaotic scattering *Phys. Rev. A* **46** 6247–51
- [24] Ding M, Grebogi C, Ott E and Yorke J A 1990 Transition to chaotic scattering *Phys. Rev. A* **42** 7025–40
- [25] Ding M, Grebogi C, Ott E and Yorke J A 1991 Massive bifurcation of chaotic scattering *Phys. Lett. A* **153** 21–6
- [26] Eckhardt B and Jung C 1986 Regular and irregular potential scattering *J. Phys. A: Math. Gen.* **19** L829–33
- [27] Fathi A 1989 Expansiveness, hyperbolicity and Hausdorff dimension *Commun. Math. Phys.* **126** 249–62
- [28] Golé C 2001 *Symplectic Twist Maps (Advanced Series in Nonlinear Dynamics vol 18)* (Singapore: World Scientific)
- [29] Holmes P 1980 Periodic, nonperiodic and irregular motions in a Hamiltonian system *Rocky Mountain J. Math.* **10** 679–93
- [30] Lai Y-C and Tél T 2011 *Transient Chaos. Complex Dynamics on Finite-Time Scales (Applied Mathematical Sciences vol 173)* (New York: Springer)

- [31] Palis J and de Melo W 1982 *Geometric Theory of Dynamical Systems* (Berlin: Springer)
- [32] Pinheiro D and MacKay R S 2006 Interaction of two charges in a uniform magnetic field: I. Planar problem *Nonlinearity* **19** 1713–45
- [33] Rod D L 1973 Pathology of invariant sets in the monkey saddle *J. Diff. Eqns* **14** 129–70
- [34] Shilnikov L P 1967 On a Poincaré–Birkhoff problem *Math. Sb.* **74** 378–97
Shilnikov L P 1967 *Math. USSR-Sb.* **3** 353–71 (Engl. transl.)
- [35] Sternberg S 1957 Local contractions and a theorem of Poincaré *Am. J. Math.* **79** 809–24
- [36] Tél T, Grebogi C and Ott E 1993 Conditions for the abrupt bifurcation to chaotic scattering *Chaos* **3** 495–503
- [37] Turaev D V 2001 Multi-pulse homoclinic loops in systems with a smooth first integral *Ergodic Theory, Analysis and Efficient Simulation of Dynamical Systems* ed B Fiedler (Berlin: Springer) pp 691–716
- [38] Turaev D V and Shilnikov L P 1989 On Hamiltonian systems with homoclinic curves of a saddle *Dokl AN SSSR* **304** 811–14
Turaev D V and Shilnikov L P 1989 *Sov. Math. Dokl.* **39** 165–8 (Engl. transl.)